Student thesis series INES nr 349

Spatially varying parameters in observed new particle formation events

Jimmie Carpman

2015
Department of
Physical Geography and Ecosystem Science
Lund University
Sölvegatan 12
S-223 62 Lund
Sweden

Jimmie Carpman (2015).
Spatially varying parameters in observed new particle formation events
Rumslig variation av parametrar i observerade nypartikelbildnings-händelser
Master degree thesis, 30 credits in *Physical Geography and Ecosystems Analysis*
Department of Physical Geography and Ecosystems Science, Lund University

Level: Master of Science (MSc)

Course duration: *January* 2015 until *June* 2015

Disclaimer

Spatially varying parameters in observed new particle formation events

---

Jimmie Carpman

Master thesis, 30 credits, in *Physical Geography and Ecosystems Analysis*

Supervisor 1:
Niku Kivekäs
Atmospheric Composition Research, Finnish Meteorological Institute, Helsinki, Finland

Supervisor 2:
Adam Kristensson
Department of Nuclear Physics, Lund University, Lund, Sweden

Exam committee:
Vaughan Phillips, Department of Physical Geography and Ecosystem Science, Lund University, Lund, Sweden

Thomas Holst, Department of Physical Geography and Ecosystem Science, Lund University, Lund, Sweden

Abstract

Aerosol particles affect the global climate due to its influence on the scattering and absorption of short-wave and long-wave radiation. The extent of the influence of aerosol particles on the climate varies a lot by time and space, and needs to be quantified. One of the most important natural sources of atmospheric particles is new particle formation (NPF). However, the contribution of NPF events on the aerosol concentrations in different regions need to be better quantified before they can be realistically described in climate models. This is of great interest due to the ongoing climate debate. Atmospheric NPF events are typically studied at stationary measurement sites, at which the observed changes in particle number concentration and size can be linked to both temporal and spatial changes in the particle formation and growth parameters, even though the spatial component is often neglected. The goal of this study is to examine how common the spatial variations in particle formation and growth parameters are, and how they affect the observed NPF events.

The method used to examine this was to first use an improved version of an existing model to simulate different NPF cases assuming spatially and/or temporally varying input parameters. From these simulations the "fingerprints" for the different parameter variations were identified. Thereafter we analyze 8 years of particle number size distribution data from measurement sites Pallas and Värriö, in Finnish Lapland, and compared the observations of NPF events to the fingerprints of the different variations in cases when the same air mass was observed at both sites.

Our results indicate that the beginning of the event is typically time dependent which could be explained by the diurnal evolution of a turbulent boundary layer. The end of the NPF event tends to be more typically dependent on location. In our observations in Northern Scandinavia this could be connected to the air mass arriving from sea to land or over the Scandinavian mountains. These findings indicate that the spatial variations of the particle formation and growth parameters cannot be neglected when analyzing NPF events.

Table of contents

1. Introduction 1

2. Background 2

2.1 Aerosols 2

2.1.1 Particle number size distribution in the atmosphere 2

2.1.2 Aerosol particle concentrations 3

2.1.3 Lifetime of aerosol particles 3

2.1.4 Geographical mixing of aerosol particles 4

2.2 Aerosol sources 4

2.2.1 New particle formation 4

2.2.2 Sea spray 6

2.2.3 Mineral dust 6

2.2.4 Biomass burning 6

2.2.5 Volcanic Aerosols 7

2.2.6 Fossil fuel combustion 7

2.3 Effects of aerosols 7

2.3.1 Climate effects 7

2.3.2 Health effects 10

2.3.3 Visibility 10

2.4 Aerosol dynamic processes 11

2.4.1 Condensation 11

2.4.2 Coagulation 11

2.4.3 Particle activation into cloud droplets 11

2.4.4 Deposition 12

2.5 New particle formation analysis 12

2.6 Assumptions made in new particle formation analysis 14

2.7 Effects of spatial variability 14

3. Methods 15

3.1 Model 15

3.1.1 Existing model 15

3.1.2 Improvements to StBanana model in this work 18

3.2 Spatial and temporal changes in simulated observations 21

3.3 Measurement sites 24

3.4 Trajectories 25

3.5 Comparison method 26

4. Results and discussion 29

5. Conclusions 32
6. Acknowledgements 33
7. References 34
9. Appendix 1: Classification of individual NPF events 40

Spatially varying parameters in observed new particle formation events

1. Introduction

Earth global climate and temperature are affected by the balance between incoming and outgoing radiation. Aerosols affect this radiative balance directly through scattering and absorption of light, and indirectly by their effects on clouds and cloud condensation nuclei (CCN). The scattering of incoming radiation has a cooling effect on the Earth's surface temperature and atmosphere, while the absorption increases the temperature in the atmospheric layer where the particles are located. The particles can also become CCN and produce clouds which effectively both absorb outgoing infrared radiation from the surface and scatter incoming solar radiation.

To be able to quantify the influence that the aerosol particles have on the climate, we need a deeper understanding of how different aerosol sources affect the population of atmospheric particles and how the particles evolve during their lifetime. Aerosol particles have many sources, and one of the most important one is new particle formation (NPF) the formation of new particles from gaseous precursors in the atmosphere.

New particle formation has been observed on every continent in the world (*Kulmala et al., 2004 and references therein*) and in very different environments from very clear Antarctic air (*Kyrö et al., 2013*) to polluted mega-cities (e.g. *Yue et al., 2010*). There have, however, only been a few studies of the regional extent of NPF events using one (*Kristensson et al., 2014*) or several measurement sites (*Komppula et al., 2006; Hussein et al., 2009; Jeong et al., 2010; Crippa and Pryor, 2013*).

Traditionally, there are several assumptions made in the usual NPF event analysis (*Dal Maso et al., 2005*). These include 1) that the formation of particles takes place at the same time in a large area, 2) the particle formation rates are the same at the measurement site and where the smallest detectable particles where formed, and 3) that the particles have the same growth rate where they were formed and at the measurement site (*Kivekäs et al., 2015*).

NPF has been studied extensively and the assumption of only time dependent formation is widely used in the research community. There is however a possibility that the formation and growth of new particles are not only dependent on the time but also on the location of the air parcel. In such a case one or more of the assumptions made in NPF analysis might be wrong.

The goal of this thesis is to investigate how common the spatial variations in particle formation and growth rate parameters are. This is achieved by first making reference simulations with a spatio-temporal NPF model dedicated for the task (*Kivekäs et al., 2015; Carpman et al., 2013*) to investigate what kind of "fingerprints" time and location dependent formation and growth will leave on the particle number size distributions at a specific site during NPF events. Then, real observations of NPF events at two measurement sites are analyzed for these fingerprints to be able to identify the different types of parameter changes in observed NPF events.

2. Background

2.1 Aerosols

An aerosol consists of small solid or liquid particles floating in a gas. The air that we breathe is an example of an aerosol. (*Hinds, 1999*). Aerosol particles vary in size and composition and are formed both naturally and from anthropogenic sources. Aerosols are involved in many different atmospheric processes and influence, for instance, both the climate and the health of humans. This will be explained below in more detail.

2.1.1 Particle number size distribution in the atmosphere

The aerosol particles in the atmosphere can have different sizes which range from only one nanometer (nm) to several hundred micrometer (µm). To better quantify these aerosol particles they are often divided into different size modes. The typically used modes are the nucleation mode consisting of particles between 1 and 30 nm, the Aitken mode ranging from 30 nm to 100 nm, the accumulation mode which spans from 100 nm (0.1 µm) to 1 µm and the coarse mode in which all particles larger than 1 µm belong to (*Seinfeld and Pandis, 2006*).

Nucleation mode (1 nm to 30 nm): The particles in this mode make up a substantial part of the total number concentration of the particles in the atmosphere but due to their small size these particles can be neglected when counting the total mass of the aerosol particles. Particles in this mode are formed by either condensation of hot vapors during combustion processes or through new particle formation in the atmosphere. Most particles in this mode are lost rapidly through coagulation with larger particles. Due to the sporadic nature of the formation processes and the effective removal processes the concentration of nucleation mode particles varies a lot in both time and space.

Aitken mode (30 nm to 100 nm): This mode together with the nucleation mode is dominating the particle number concentration. However, the Aitken mode (and the nucleation mode) do not account for more than a few percent of the total mass of the airborne particles in the atmosphere. Particles in the Aitken mode originate from either particles that have grown from the nucleation mode into the Aitken mode through condensation, or during direct emissions of particles in this size range. The smallest particles in this size range are removed from the atmosphere through coagulation, while the largest ones can transfer to the accumulation mode through condensational growth or even through cloud activation.

Accumulation mode (0.1 µm to 1 µm): This is a large mode particularly when considering the total mass or surface area of the aerosol particles. The name accumulation mode originates from the fact that particles accumulate in this size range, due to the removal mechanisms for this size range being less effective than for smaller and larger particles. Due to the ineffective removal, the particles in the accumulation mode have considerably longer lifetimes than particles in the other modes.

Coarse mode (>1 µm): This mode consists of mainly particles from mechanical processes such as windblown dust, sea spray particles during wave breaking, natural grinding, volcanic activity and human-made dust particles from wearing down asphalt, car tires, car breaks from vehicle traffic and other mechanical grinding from human activities. Particles in the coarse mode have short residence time in the atmosphere due to effective removal by dry deposition (*Seinfeld and Pandis, 2006*).

2.1.2 Aerosol particle concentrations

Different environments can have very different aerosol concentrations.

Urban areas: The particle number concentration in this type of environment is dominated by particles smaller than 0.1 µm whereas the mass concentration is dominated by particles larger than 0.1 µm. The particle number concentration is about an order of magnitude larger close to large roads compared to average urban particle concentrations. A typical number concentration in urban areas is around 10^5 cm^{-3} (*Seinfeld and Pandis, 2006*). In many cities the mass of particulate matter with diameter smaller than 10 µm (PM10) is between 20-60 $\mu g/m^3$, but in some megacities like Beijing measurements of higher than 900 $\mu g/m^3$ have been recorded (*World Air Quality Index, 2015*).

Rural areas: Aerosols in rural areas comes from both natural as well as anthropogenic sources. The number concentration in this type of environment is typically about 4000 cm^{-3} or less and the accumulation mode is the largest mode. The PM10 concentration is normally between 10 and 20 $\mu g/m^3$ (*Putaud et al., 2004*).

Background areas: In remote areas that are only weakly influenced by anthropogenic activities the typical particle number concentrations vary from few tens to a few thousands of particles per cm^{-3}. In such areas the main particle sources are naturally occurring new particle formation events and long-range transport of Aitken and accumulation mode particles (*Tunved et al., 2006*).

Free troposphere: The free troposphere refers to the mid- and upper troposphere which is located above the cloud base height and is unaffected by the boundary layer. In this part of the troposphere the particle concentrations are lower than at the surface, and the particle size distribution is more concentrated in the accumulation mode. This is due to the fact that particles are effectively lost only through precipitation scavenging in the free troposphere (*Leaitch and Isaac, 1991*). The low temperatures and the low total particle surface area makes free tropospheric air also suitable for new particle formation and thus the nucleation mode is often present in the number distribution. The typical particle number concentration in the free troposphere is below 1000 cm^{-3}, but can rabidly increase to tens of thousands per cm^{-3} during new particle formation events. The PM value is around 1 $\mu g/m^3$ (*Seinfeld and Pandis, 2006*).

2.1.3 Lifetime of aerosol particles

The lifetime of aerosol particles is much shorter than the lifetime of greenhouse gases, and therefore the aerosols are referred as short-lived climate forcers. For instance the lifetime of carbon dioxide is 35-95 years (*Jacobson, 2005*) and methane has a lifetime of approximately 10 years (*IPCC, 2001*). The lifetime of atmospheric particles with diameter less than 10 nm or larger than 20 µm is on average less than one day. The lifetime of particles belonging to the accumulation mode is, however, longer due to less effective removal mechanisms and can be up to several weeks (*Wallace and Hobbs, 2006*).

2.1.4 Geographical mixing of aerosol particles

Due to the short particle lifetime the geographical mixing of aerosol particles is highly variable and has a strong connection to particle sources. This means that there are places where the concentration of aerosol particles is extremely high and very harmful to humans, for example in mega-cities like Beijing, and places where the concentration is very low, such as Polar Regions or the free troposphere.

2.2 Aerosol sources

The aerosol particles can be divided into two groups based on the nature of their source. The primary particles, which are emitted directly to the atmosphere, and the secondary particles, which are formed in the atmosphere through gas to particle conversion. This division is, however, not very clear, as secondary material accumulates over time also on primary particles in the atmosphere through condensation, which is explained below.

Primary particles are produced from combustion processes, from mechanical grinding or from biological activity. Some of the important combustion sources are biomass burning, volcanoes and anthropogenic sources like vehicle engine combustion, and coal power plants. Particles produced from mechanical grinding are sea spray, mineral dust, and particles produced from transportation. The important biological particles are pollen, bacteria, fungal, spores, viruses, algae and biological crust.

Secondary particle sources can be divided in two different groups, condensation of gases on already existing particles and new particle formation from gaseous precursors.

The main aerosol sources are described below in more detail.

2.2.1 New particle formation

Aerosol formation in the atmosphere, also called new particle formation (NPF), is a major source of aerosol particles. It is also the main focus of this work. In the process of NPF the particles nucleate from precursor species in the gas phase and the nucleation process is followed by a rapid growth of the particles by condensation. The nucleation and growth of the newly formed particles are believed to be two different processes driven by different chemical species (*Kulmala et al., 2013*). The theory of NPF including nucleation and initial growth is not yet accurately described due to a lack of complete understanding of the phenomena and limited capability of measuring particles with diameter below 3 nm (*Kulmala et al., 2013*). However, the derivations of nucleation rates and growth rates can be obtained from empirical studies with certain assumptions.

The classical way of viewing new particle formation is through homogeneous kinetic nucleation, through homogeneous binary water-sulfuric-acid nucleation, or through ternary water-sulfuric-acid-ammonia nucleation (explained in *Kristensson and Martinsson, 2015*). In all these theories, sulfuric acid is one of the main agents in new particle formation, and we have an interaction between two or several molecules of the same type when forming a stable particle cluster, why this is termed as homogeneous. During the last years, heterogeneous nucleation of neutral or ion clusters has been the dominating theory for NPF. It involves the activation of nucleated clusters by a sulfuric acid molecule, which makes the cluster stable without the possibility to break up again. The term heterogeneous comes from the fact that the

cluster participating in the formation can contain a multitude of different species. The formation of the stable clusters takes place around 1.5 nm diameter according the latest consensus in the field (Kulmala et al, 2013).

The formation rate ($J_{1.5}$) is the rate at which new stable clusters are formed at 1.5 nm. This rate is determined by the presence of chemical species with low vapor pressure. Sulfuric acid, ammonia and different organics, for instance amines, are the important chemical species involved in atmospheric nucleation (*Kulmala et al., 2013*).

To be able to estimate the growth of the nucleated particles and their effect on the aerosol number size distribution, the loss of particles through coagulation and the loss rate of condensing vapors onto pre-existing particle surface have to be taken into account. For both of these reasons, NPF events are rarely observed in the presence of a large accumulation mode because the stable clusters will more likely coagulate on the existing particles than grow to larger sizes through condensation, and the condensable vapors are more likely to condense on the surface of the pre-existing particles than on the newly formed ones. These phenomena can prevent the entire NPF event, but can also lead to loss of the newly formed particles due to coagulation before they have grown to a measurable size.

Figure 1 shows an example of a NPF event from the Vavihill field station located in southern Sweden. In this figure one can see how the mode of newly formed particles around 3 nm in diameter is growing due to condensation and reaching a size of around 30 nm in diameter by the end of the day. This growth appears as a banana-like shape in the plot with logarithmic diameter axis, and is therefore often referred to as a "NPF banana".

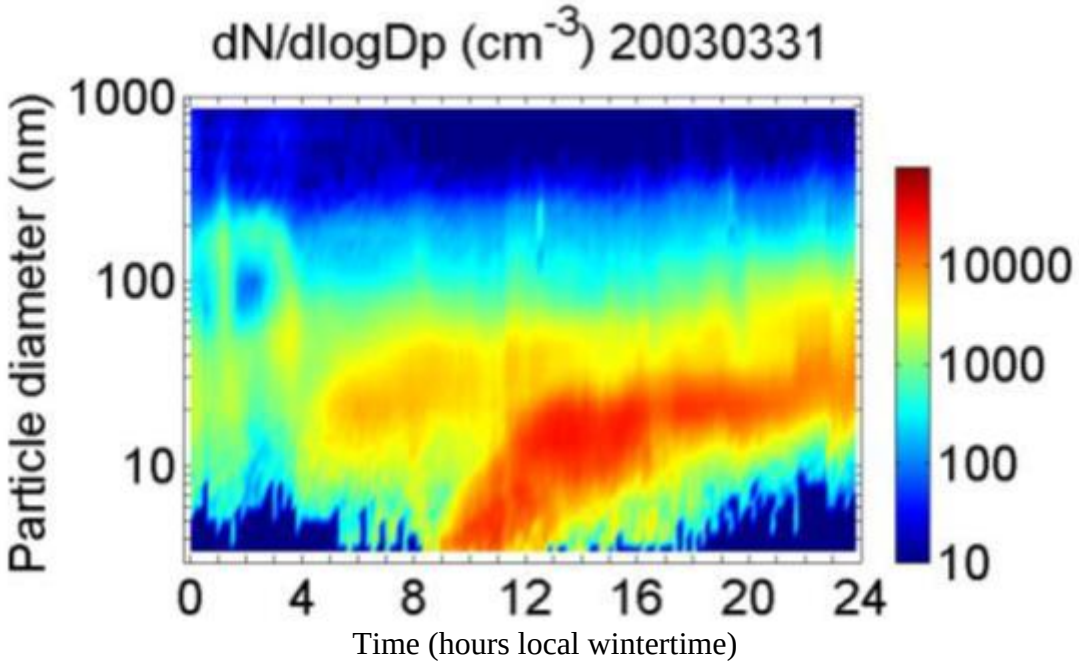

Figure 1: Particle number size distribution measured at the Vavihill field site during the last day of March, 2003. The x-axis is local wintertime, the y-axis is the particle diameter in logarithmic scale and the color scale is the number concentration as $dN/d\log_{10}D_p$ in cm^{-3}.

2.2.2 Sea spray

Aerosol particles which have their source from the ocean are called sea spray. They are formed through bubble bursting which is mostly associated with wave breaking. The surface wind speed, the atmospheric stability, the sea state, and also to a lesser extent the temperature and salinity of the sea water are the determining factors for the emission rate of sea spray particles. The understanding of sea spray emissions have increased during the last couple of years but estimates of total mass and size distribution, which are process-based, have still large uncertainties (*de Leeuw et al., 2011*). The aerosol particles that are created through sea spray processes consist of salt and marine primary organic matter. In most cases the marine primary organic matter is present in particles with diameter smaller than 200 nm. The marine organic aerosol emissions depend on the biological activity in the ocean water and the emission estimates in a global scale range from 2 to 20 Tg yr^{-1}. The particles larger than 200 nm originates primary from sea salt and have total global emission estimates from 1000 to 3000 Tg yr^{-1} (*IPCC, 2013*).

2.2.3 Mineral dust

The main production mechanisms and sources of mineral dust particles are the disintegration of larger dust particles when the particles are creeping and saltation over desert floor or other arid surfaces. The magnitude of dust emissions varies depending on the surface wind speed, the texture and moisture of the soil, and the vegetation cover. *Huneeus et al., 2011* estimated that the global dust emissions vary by a factor of five. For instance in North Africa the emission vary between 400 to 2200 Tg yr^{-1}.

Another source of mineral dust is anthropogenic emissions. Transportation, when excluding the particles from combustion engines, is an important source of particles formed though mechanical grinding. The particles are produced when the car tires are in contact with the road. The wearing down of the asphalt by the tires deposits particles on the road surface. As the road surface becomes dry, these deposited particles have a chance to become airborne through the wind acting on the road surface or through the turbulence generated by the moving vehicles. The land use change created from agricultural activities will create emissions of mineral dust particles from agricultural areas, when these are not covered by growing plants.

The contribution of the anthropogenic emissions has been estimated to stand for 20 to 25 percent of the total mineral dust emissions (*Ginoux et al., 2012a, 2012b*).

2.2.4 Biomass burning

There are basically two major components in biomass burning aerosols. These are black carbon and organic carbon. Black carbon is a good absorber of solar radiation whereas organic carbon scatters solar radiation effectively. The sources of biomass burning aerosols are burning of forests, savannas, agricultural waste and other substances burned for fuel such as wood, dung and peat. Most of the emissions from large forest fires are detected through satellite data. Due to poor sensitivity of the satellite data the data from small fires are mostly missing which leads to higher uncertainty (*IPCC, 2013*).

2.2.5 Volcanic Aerosols

Volcanos are important natural source of particles in the atmosphere. Most of the aerosol particles emitted from volcanic eruptions consist of sulfur dioxide and ash. The sulfur dioxide converts to particulate sulfuric acid which is effective at reflecting radiation and thus cools the climate. If the eruption is explosive and the sulfur dioxide enters the stratosphere the particles can stay in the atmosphere a couple of years and the impact on the climate will be longer lasting and cover a larger area (*McCormick et al., 1995*). The ash particles are effective at absorbing radiation and if located on a bright surface, e.g. snow, the ash will have a warming effect.

Measurements from the eruption of Eyjafjallajökull in 2010 showed a broad range of emissions at different particle sizes. Depending on the phase of the eruption the particles emitted were fine particles (<1 µm) or particles belonging to the coarse mode (*Ilyinskaya et al., 2011*).

2.2.6 Fossil fuel combustion

A large fraction of the anthropogenic aerosol particles originates from combustion engines in cars, ships, air planes and so on. The particles from this source belong primarily to the nucleation mode and the Aitken mode in the number concentration but in the mass concentration the accumulation mode is largest.

Coal power plants and coal combustion in general emit large amount of particles. Most of these particles are in the form of coal ash and soot. The particles emitted belong to all modes, even though only one percent of the total mass is observed in particles with diameter (D_p) < 0.5 µm (*Linak et al., 2006*).

2.3 Effects of aerosols

2.3.1 Climate effects

Aerosols can influence the climate by both warming and cooling the atmosphere in comparison with greenhouse gases which only heat the atmosphere and thus the climate. The change in the energy trapped in the earth and atmosphere system today compared to the preindustrial period (1750) is defined as the radiative forcing. Such changes are caused by changes in radiative forcing drivers, of which one is aerosol particles (*IPCC, 2013*). The aerosol particles can influence the radiative balance in two different ways; via the direct and the indirect effects (figure 2).

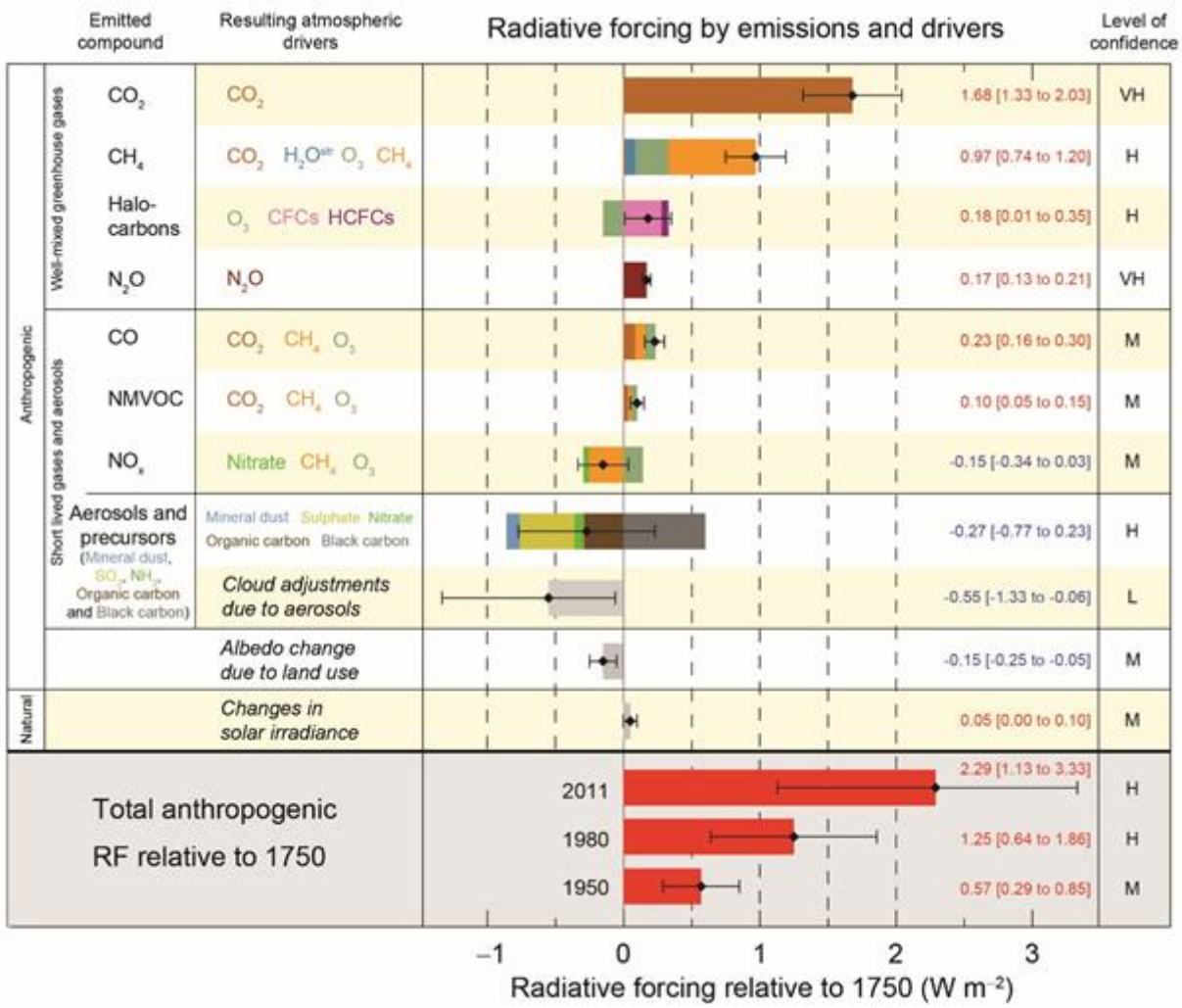

Figure 2: Present day radiative forcing caused by different components and relative to pre-industrial time (*IPCC, 2013*). The direct effect of aerosols is denoted with the respective forcing change for different types of aerosol particles separately (Mineral dust, sulfate, nitrate, organic carbon, and black carbon). The indirect effect of aerosols is denoted with "Cloud adjustments due to aerosols". Both of these have large uncertainties, visualized with the error bars.

The direct effect refers to the change in scattering and absorption of both shortwave and longwave radiation by aerosol particles. The optical properties of the aerosols are the most important parameters to determine their direct effect. The optical properties vary depending on the wavelength of incoming radiation, the relative humidity, the concentration of particles, the chemical composition of the particles and the particle size distribution. (*Haywood and Boucher, 2000*). Aerosol particles that scatter incoming solar radiation induce a negative radiative forcing independent of the type of surface that are underneath while aerosol particles that can absorb light may induce both a negative radiative forcing and a positive radiative forcing depending on the surface underneath. If the surface is dark, such as an ocean or forest, the absorbing aerosols exerts a negative radiative forcing, but if the surface is light like a desert or ice they will have a positive radiative forcing. Independent of positive or negative direct radiative forcing the effect at the surface is the same, which is a negative total radiative forcing. For the longwave direct effect to be substantial the concentration of aerosol particles

needs to be high, the sizes of the particles need to be large and the aerosols need to be located at high altitudes (*IPCC, 2013*).

The indirect effect of aerosol particles is the effect which anthropogenic aerosol particles exert on the radiative properties, amount, and lifetime of clouds. The effectiveness of an aerosol particle to influence radiative forcing through the indirect effect is its ability to act as a cloud condensation nucleus (CCN). The effectiveness is determined by the particle size, chemical composition, mixing state, and ambient environment (*Penner et al., 2001*). The first indirect effect is the effect that aerosols have on the cloud droplet number concentration and thereby also the cloud droplet size when the liquid water content is held at a constant level (*Twomey, 1974*). This is also called the cloud albedo effect due to the change in cloud brightness. Compared to an unperturbed cloud influenced by natural aerosol particles only, a cloud influenced also by anthropogenic aerosol particles has a larger number concentration of aerosol particles and therefore also larger number concentration of potential CCN. This leads to a larger number of cloud droplets competing for the same amount of water. As a result the droplets remain smaller but are greater in number, creating larger total droplet surface area compared to an unperturbed cloud. The larger surface area leads to more effective scattering of solar radiation. The second indirect effect (*Albrecht, 1989*) is also called the cloud lifetime effect and consists of three parts, the liquid water content, cloud height and lifetime of clouds. The decreased droplet size leads to less water being lost in form of drizzle, thus increasing the liquid water content in the cloud. The increased water content of the cloud makes the cloud thicker which increases the cloud top height and the reflection of light back to space. However, it may also have a warming effect through the "blanketing" effect, meaning that with thicker clouds and longer cloud lifetimes the loss of heat to space is also reduced. With increased water content and cloud height the lifetime of the cloud will increase and exert its cooling or warming effects for an extended period of time compared to natural unperturbed clouds. (*IPCC 2013*).

An illustration of the direct and indirect effects are shown in figure 3.

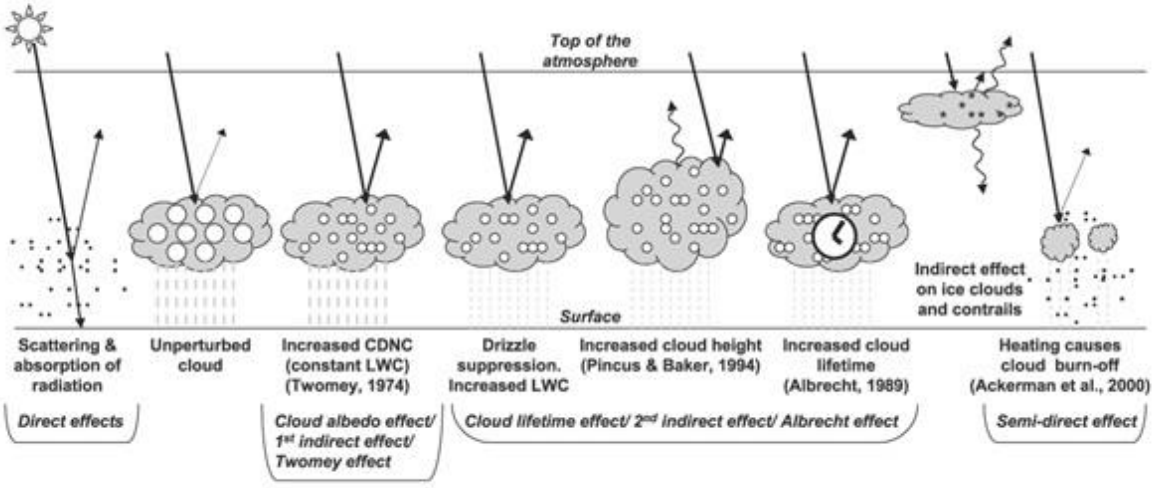

Figure 3: The direct and indirect climate effects of aerosol particles in the atmosphere (*IPCC, 2007; Twomey, 1974; Pincus and Baker, 1994; Albrecht, 1989; Ackerman et al., 2000*).

2.3.2 Health effects

A significant impact of aerosol particles on human health has been observed trough epidemiological research. The aerosols that have been identified to possess the greatest impact on human health are found in the size range of fine particular matter (PM-10 and PM-2.5) (*Samet et al., 2000*).

Mortality from aerosol pollution is calculated by removing the known causes of mortality from diseases, accidents, etc. and after removing these there is a few percentage left which cannot be explained this way. This percentage has a good correlation with air pollution. With a more detailed investigation made in Europe and United States there was a significant correlation with the concentration of fine particles (PM-10 or PM-2.5) and the mortality. The excess mortality has been traced for different location and it varies depending on location and the effect seems to be linear with the concentration of fine particles. No threshold for the aerosol-induced excess mortality has been found (*Buringh and Opperhuizen, 2003*). For instance there is evidence that ship related PM emissions are responsible for many premature death globally. These deaths are mainly in coastal regions of Europe, East Asia and South Asia where shipping activities are high, but also in inland population centers due to long range transport of pollutants. According to *Corbett et al., 2007* the ship emissions of PM result globally in approximately 60 000 death annually and they believe this number to increase dramatically in the coming years.

2.3.3 Visibility

The impact that aerosol particles can have on visibility is large and it depends on the size and number concentration of the particles as well as relative humidity. The reason why aerosol particles impact visibility is that we see an object only due to light reflected from it. Aerosol particles reflect or scatter the light in front of the object limiting the distance how far we can see, also known as visibility. Aerosol particles limit the visibility trough two different pathways. The first one is that the amount of light emitted by /reflected from the object is reduced before arriving at the observer. The second pathway is that light from other sources is scattered by the aerosol particles creating a background haze, and the scattered light, can also reach the observer from the direction of the object. The size of the particles for maximum impact on visibility is between 0.1 and 2 μm (*Slanina, 2012*).

The scattering affecting the visibility can be described through two theories depending on the size of the scattering particles. These are called Rayleigh scattering and Mie scattering.

Rayleigh scattering occurs when the sunlight is scattered by gas molecules. This scattering theory (*Strutt, 1871*) states that the amount of light scattered is inversely proportional to the fourth power of the wavelength of the light (λ^{-4}). With decreasing wavelength of the incoming light, more light is scattered. This relationship is only valid when light is scattered by small particles or gas molecules. The sky is blue due to the Rayleigh scattering, since blue light is scattered more intensely. For the same reason sunrises and sunsets are red due to all the blue light already being scattered earlier in the atmosphere (*Rayes, 1997*).

Mie scattering occurs when the wavelength of the light and the size of the particles are of the same order. To be able to apply Mie scattering theory on aerosol particles they need to be spherical, which is the case with for instance, cloud droplets. This is why clouds are often white, the cloud droplets scatter all the visible light in all directions (*Rayes, 1997*).

2.4 Aerosol dynamic processes

2.4.1 Condensation

When the vapor pressure of a gas exceeds the saturation vapor pressure required for the absorption of gas molecules onto an aerosol particle, the gas starts to condense on the particle surface. Different gases have different saturation vapor pressures. A lower value makes it easier for the gas to condense and reach the particle phase (*Seinfeld and Pandis, 2006*). Many organic and inorganic compounds possess a low enough saturation vapor pressure needed for condensing onto an aerosol particle in ambient atmospheric conditions. The aerosol particles can grow rapidly due to condensation when high concentrations of these compounds are available. This increases the particle mass and volume, but can also alter the chemical composition of the particles. There can be thousands of different compounds in a single particle depending on the chemistry of the surrounding air during the formation and growth processes.

2.4.2 Coagulation

As the particles in the aerosol collide they can undergo coalescence or aggregation. The number size distribution of the aerosol particles is affected by this and the result of this will lead to the growth in size and a decrease in number concentration of the particles. (*Hinds, 1999*). The rate at which the particles coagulate depends mainly on the particle number concentration and size. Smaller particles have higher speed and move more randomly which gives them a higher possibility to collide with larger particles which have a larger inertia and a larger surface area (*Hinds, 1998*). This will lead to the highest number of collisions between particles with large difference in size.

The coagulation process is very effective at removing small particles and therefore act as a sink for particles belonging to the nucleation mode and the Aitken mode. (*Kerminen et al., 2004; Seinfeld and Pandis, 2006*).

2.4.3 Particle activation into cloud droplets

In an atmosphere devoid of particles the relative humidity would need to be several hundred percent in order for any water droplets to form. Particles in the atmosphere are therefore essential for the formation of clouds and rain. Particle activation into cloud droplets depends on four things: the particle size, the chemical composition of the particle, the physical structure of the particle and the super saturation of water vapor in the air. The definition of super saturation is the part of relative humidity exceeding 100 percent. Similar to the critical cluster diameter in nucleation process, also in cloud droplet activation the particle must exceed a critical activation (wet) diameter in order to activate. A particle that is activated can grow in size spontaneously into a cloud droplet. To be able to form clouds we need particles that can act as CCN and a relative humidity higher than 100 percent (*Seinfeld and Pandis, 2006*).

Condensation of water on particles takes place even if the relative humidity is less than 100 percent. In this case the size of the droplet depends on the amount of water-soluble material in the droplet and on relative humidity. This means that if the relative humidity decreases the droplet will shrink by evaporation and if the relative humidity increases the droplets will grow by condensation. (*Frank, 2001*).

2.4.4 Deposition

Deposition is a process which removes particles from the atmosphere. There are two types of deposition: dry and wet deposition.

Dry deposition is when particles are transported from the atmosphere and deposited to different surfaces without precipitation. The factors that determine the effectiveness of the dry deposition process are the physical and chemical characteristics of the particles and the surface, as well as the amount of turbulence in the air. The amount of atmospheric turbulence determines how much of the particles that come in contact with the surface. The factors that determine if the particles will be captured by the surface are the size, shape and density of the particles. The type of surface is also important for the dry deposition. The deposition is more effective if the surface has large and uneven obstacles. Dry deposition is most effective for small particles due to their random Brownian motion, and for big particles due to their larger inertia and decreased capacity to follow air motion in the turbulence (*Seinfeld and Pandis, 2006*).

Wet deposition is the removal of particles from the atmosphere by atmospheric hydrometeors. Hydrometeors include cloud droplets, rain drops, fog droplets, snow crystals etc. The wet removal processes have different names depending on which hydrometeors are involved. For instance, wet deposition is called in-cloud scavenging when aerosol particles are removed by activation into cloud droplets which then form rain droplets that precipitate out of the clouds. The wet deposition is called washout when particles located underneath the clouds are removed by the falling rain drops as they collide with the airborne particles. A common name for all these processes is wet removal.

Almost all of the wet removal processes are reversible until the particles are deposited on the surface of the earth. For instance if a particle is captured by a rain droplet the reversal of this process is evaporation of the droplet, this will release the aerosol particle to the atmosphere again.

2.5 New particle formation analysis

In measurements of aerosol particles there are no observation of the newly formed particles through remote sensing due to the lack of capability to observe such small particles with these techniques. The information obtained on formation and growth of the particles in ambient atmosphere is attained mostly from measurements at fixed locations. By conducting measurements in this way we are not observing the evolution of the same particles, but we are instead observing a new set of particles on each measurement cycle. This should be taken into account on the analysis of NPF events.

Since new particle formation occurs frequently in the atmosphere we need information about the time when NPF events were recorded and when no event were present, in order to

determine the processes and atmospheric conditions leading to NPF events. By using this information it is possible to correlate atmospheric variables with NPF events. An exact criterion for NPF is not agreed upon (*Dal Maso et al., 2005*). There are, however, some criterion used in NPF analysis to classify measurement days to either event days or non-event days. The criteria are:

1. A clear formation of a new mode of particles must appear in the size distribution.
2. The new mode must start in the nucleation mode size range.
3. The new mode must prevail over a time span of hours.
4. The mode has to show signs of growth.

By using these criteria one can exclude new particle formation from point sources like local pollution or heating. The fourth criteria where it states that all NPF events has to grow, is needed due to the fact that the formation size of the new particles is smaller than what we can measure. Growth is therefore required to be able to measure the particles at all (*Dal Maso et al., 2005*)

In NPF analysis it is convenient and mathematically straightforward to represent the size distribution in log-normal modes. The size distribution of the modes is described as the sum of *i* modes with the parameters: geometric diameter (D_{pgi}), geometric standard deviation (σ_i) and number concentration (N_i). In experimental conditions with measured size distributions one can use an automatic fitting method (*Hussein et al., 2005*) to find these parameters. The fitting program finds the number of modes by analyzing the size distribution.

A critical part of NPF events are when the new particles grow to larger sizes through condensation. The critical factors are:

1. The increase in size of the new particles from the growth process makes them less prone to be removed by inter- and intramodal coagulation.
2. The new particles might grow in size and can reach the Aitken mode and even the accumulation mode, at which they are likely to participate in cloud formation processes.
3. The growth by condensation removes condensational vapors from the atmosphere which could be a control mechanism to prevent additional particle formation.

The growth rate is obtained by fitting a first-order polynomial to the geometric mean diameters of the nucleation mode from the log-normal fitting in the beginning of the formation. The formation rate of new particles is harder to derive because of the limitation of the instruments which make it impossible to measure the particle at the size of formation. To derive the formation rate one need to focus on the flux of particles entering the observable size range (*Dal Maso et al., 2005*) and the loss rate of particles due to coagulation before they reach the measurable size (*Lehtinen et al., 2007*).

2.6 Assumptions made in new particle formation analysis

There are some assumptions made in NPF analysis of the NPF events that show signs of growth for at least several hours (*Kivekäs et al., 2015 and references therein*):

1. The particle formation takes place simultaneously over a large geographic area (*Hussein at al., 2009*).
2. The NPF rates are the same at the measurement site and where the smallest observed particles where formed.
3. The particles grow simultaneously and with the same growth rate within the region of formation.

With these assumptions we know that in each new measurement cycle the set of particles measured has been formed slightly further upwind from the measurement site than the previous set of particles. This results in larger particles in each new set measured. We can calculate the growth rate of the new particle mode based on assumptions 1 and 3 (*Leppä et al., 2011*). This also means that if there are particles in the smallest size class in the new set of particles measured, the formation of new particles needs to be present at or very near the site. This allows us to calculate the formation time period (e.g. *Kristensson et al., 2014*). Calculation of the new particle formation rate is possible, based on assumption 2 and 3, by using the number concentration in the new mode. This calculation is only accurate if the particles lost during initial growth can be quantified (the growth of the particles between the formation size and the size of first observation, *Dal Maso et al., 2005*). With the combination of the evolution of the new particle mode and trajectory data it is possible to calculate where the particles from observation were formed between 1 and 2 nm diameter, and thus to know the extent of the formation area upwind of the station according to assumption 1 and 3 (*Hussein et al., 2009; Kristensson et al., 2014*).

2.7 Effects of spatial variability

NPF has been studied extensively and the assumption of only time dependent formation is widely used. There is however a possibility that the formation and growth of new particles are not only dependent on the time but also on the location of the air parcel. In such a case one or more of the assumptions made in NPF analysis might be wrong.

If the formation and growth of new particles is only time dependent the NPF banana detected at the measurement site will be continuous between the smallest observable sizes and larger sizes, and the observed changes in the growth rate of the banana correspond to changes of particle growth rate at the measurement site. If the parameters are also location dependent, the observed particle population at the measurement site can show effects that are not at all connected to what is happening at the site, but to phenomena taking place hundreds of kilometers away. In such case the analysis of formation and growth parameters of the newly formed mode can lead to erroneous results (*Kivekäs et al., 2015; 2014*).

3. Methods

3.1 Model

3.1.1 Existing model

The original model that was used in this work was the StBanana model created by *Carpman, 2013* and improved by *Kivekäs et al., 2015*. This model is a one-dimensional row of Lagrangian moving boxes along a hypothetical air trajectory ending at a hypothetical measurement station where the particle number size distribution is saved. The interval of the boxes is defined such that each box starts at a distance equivalent of 10 minute advection upwind from the measurement station. This leads to the boxes arriving at the site with 10 minute intervals. The model uses 48 hours of simulation which results in 288 boxes of air. The saved result in this setup is a similar evolution of particle number size distribution to what a stationary field measurement station would register in the field. This approach gives the user the opportunity to compare real measurements to the simulated ones involving user-defined wind speed, growth rates and formation rates (*Carpman, 2013*). An illustration of the movement of the boxes and how the corresponding observations will look like at the hypothetical measurement site can be seen in figure 4.

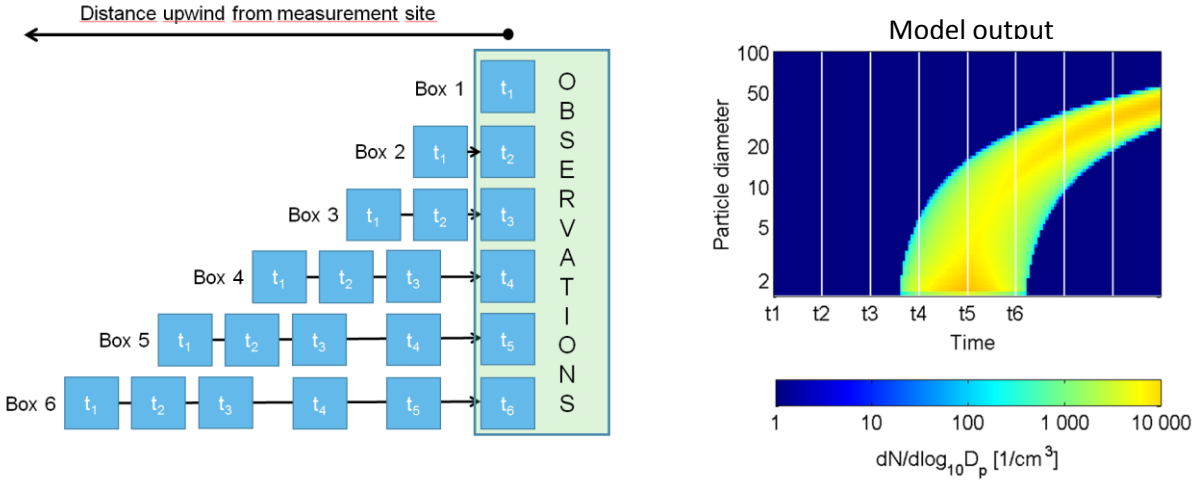

Figure 4: An illustration of how the row of moving boxes end up at the measurement site (left) and how the observation will look like (right). The t_i values represent time step i (*Kivekäs et al., 2015*).

Input parameters in StBanana are wind speed (*WS*), growth rate of particles (*GR*) and formation rate of new particles at 1.5 nm diameter ($J_{1.5}$). The wind speed can be constant or a function of time, and is used only for calculating the positions of each box at each time step. The calculation is done backwards from the station.

The input of growth rate (GR) is both time and location dependent and is defined as:

$$GR(t,x) = T_{GR}(t) \cdot S_{GR}(x) \cdot 1\frac{mm}{h}$$

Where T_{GR}(t) is the temporal input parameter and S_{GR}(x) is the spatial input parameter. The growth rate in this model represents only the growth of the particles due to condensation.

The input of formation rate ($J_{1.5}$) is similar to the input of growth rate consisting of a time dependent and a location dependent parameter. The equation is defined as:

$$J_{1.5}(t,x) = T_{J1.5}(t) \cdot S_{J1.5}(x) \cdot \frac{1}{cm^3 s}$$

Where $T_{J1.5}$(t) is the temporal input parameter and $S_{J1.5}$(x) is the spatial input parameter.

The user also has the choice to include or exclude Brownian coagulation. The coagulation is only treated as a sink for particles smaller than 150 nm in diameter.

The user inputs have an effect on formation of new particles, growth of the particles through condensation and loss of particles due to coagulation, which all alter the particle number size distribution and concentration in the boxes.

The time step for the boxes and the input parameters is 10 minute. In order to adequately describe the competition between dynamical processes affecting the particle number size distribution the calculations of these processes is done with a time step of 1 minute.

In the model the formation of new particles is treated by simply adding a new particle bin at diameter 1.5 nm to each box at every 1-minute time step when $J_{1.5}$(t,x) is larger than 0. The higher the value of $J_{1.5}$(t,x) is, the larger is the number of particles added to that size bin. After the potential creation of the new bin the particles in all bins undergo condensational growth. The growth is simulated by simply increasing the size of the particles in each bin in the box by a number defined by *GR*(t,x). The growth is only applied to particles smaller than 150 nm in order to keep the condensational sink constant throughout the simulation. In the final step of the simulation, the coagulation is calculated. The coagulation acts only as a sink for particles in the model; the particle diameters in the bins do not change and no new bins are created due to coagulation (*Kivekäs et al., 2015*).

The output of the model is presented as d*N*/dlog$_{10}$(*D*p) and the particle number size distribution in the box of air is fitted to this format. The particle mass and number concentration are preserved during the fitting. The particle number size distribution is saved in an output file for each box at the hypothetical measurement station. The saved data mimics ambient measurements at a fixed field measurement site.

Using the data from the particle number size distribution and the revised Kerminen-Kulmala equation (*Lehtinen et al., 2007*) the formation rate at 1.5 nm diameter is calculated from the simulation output data. This calculation is not precise due to the fact that neither the Kerminen-Kulmala equation nor the handling of coagulation in the model is exact. The formation rate is calculated twice, based on particle number concentration at both 5 nm and at 10 nm. The growth rate is also calculated in two different ways using the output data, first by following the peak of the mode as a function of time and the second method by following the time when maximum particle number concentration is reached for each size bin.

A figure presenting the time evolution of the particle number size distribution as a number-size-time plot at the measurement station is also made (figure 5). This figure also includes the evolution of total number concentration of particle smaller than 150 nm as a function of time ($N_d \leq 150$ nm), the particle formation rates ($J_{1.5}$) and growth rates of the observed mode (GR) at the station and the corresponding $J_{1.5}(t,x)$ and GR(t,x) at the station calculated from the input parameters. Finally the input parameters (WS, $T_{J1.5}(t)$, $S_{J1.5}(X)$, $T_{GR}(t)$, $S_{GR}(X)$) are also included in the figure (*Kivekäs et al., 2015*).

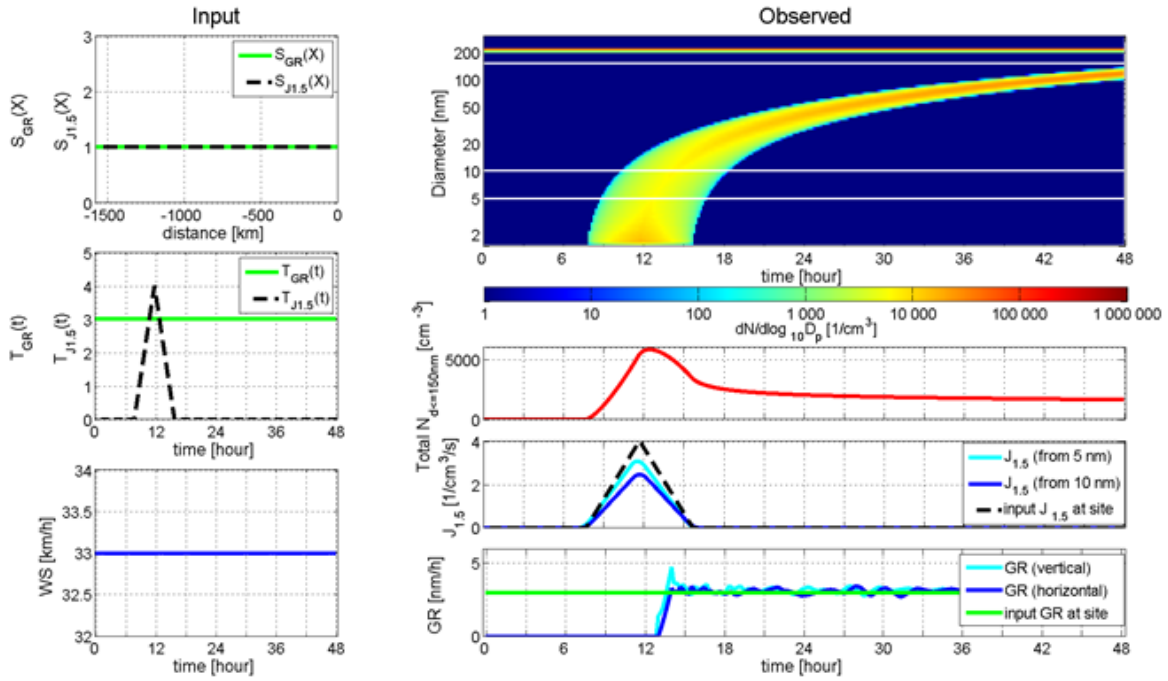

Figure 5: (from *Kivekäs et al., 2015*) Plot of a new particle formation event in the StBanana model output. This event is limited only temporally ($T_{J1.5}(t) > 0$ between hours 08 and 16, all other parameters are constants). The left panels show the input values for $S_{J1.5}(X)$, $S_{GR}(X)$, $T_{J1.5}(t)$, $T_{GR}(X)$ and *WS*. On the right side, the top panel shows the evolution of particle number-size-distribution as a function of time for two days, with particle number concentrations in each bin given as color in $dN/d\log_{10}D_p$. The second panel shows the number concentration of particles with $D_p < 150$ nm as a function of time. The third panel shows the formation rate, $J_{1.5}$, as calculated from the output particle number size distribution data and as given in the input values. Finally, the bottom panel shows particle growth rates as a function of time calculated from the output particle number size distribution data and the input growth rate at the measurement site as a function of time.

3.1.2 Improvements to StBanana model in this work

To get a deeper understanding and also to allow simulations of more realistic cases some changes were made to the original StBanana model in this work.

First, major changes to the way of setting the input values were made. The input was made more realistic by making the time- and location dependent variables truly independent of each other. This required input of the variables as a matrix. The user now has for both formation rate and growth rate the choice between a constant value and input as a matrix where the time- and location dependent components of the input parameter are presented on the different axis. These changes were made to the input of formation rate and growth rate while the input for wind speed remained as before. In figure 6 one can see the new procedure of setting the input for formation rate. The matrix input for growth rate is made the same way.

First step of the input is shown in figure 6A where the user selects the shape of the polygon in which the formation rate has positive non-zero values. Outside the polygon the formation rate is zero. In the second step of the input the user selects a value for the formation rate and then clicks inside the polygon to set points where the formation rate has that value, which is illustrated in figure 6B. This can be done multiple times with different values to set up the simulation the user desires. When the input values are set the program interpolates values from the selected points to each other and to the zero values at the edge of the polygon. The resulting formation rate matrix is shown in figure 6C.

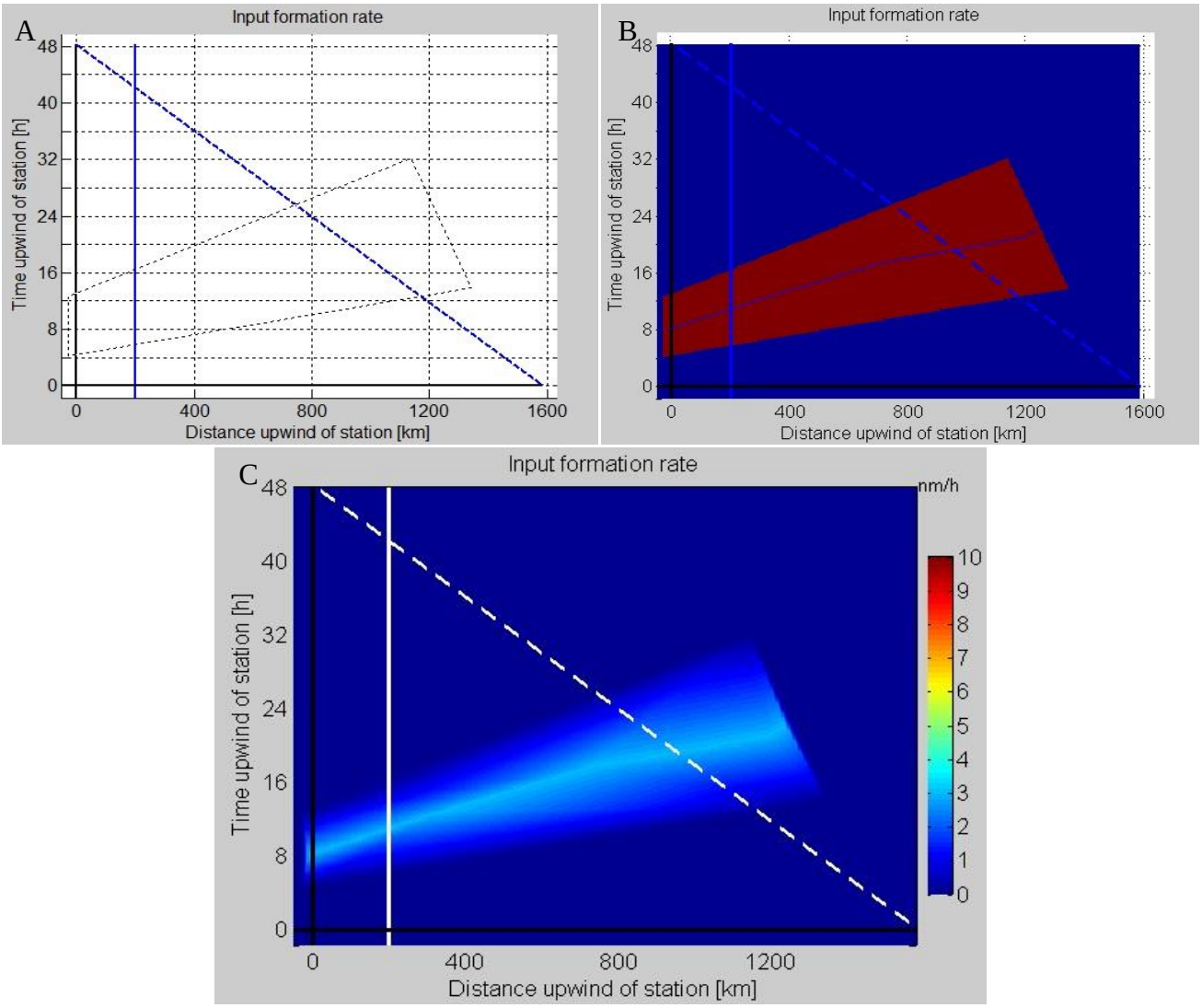

Figure 6: The input for formation rate. The vertical blue line (white at stage C) represents the upwind station and the diagonal dashed line is the limit distance where anything right of the line does not have time to arrive at the measurement site before the end of the simulation. A) Here one selects the shape of the polygon in which the values are above zero. B) Setting the non-zero values and their location in the input matrix. C) The resulting formation rate matrix.

Second, a second measurement site was added upwind of the first one. This allows the user to have the possibility to see how the particle number size distribution changes during the transport between the two stations and also to make the separation of the effects of time-dependent and location-dependent changes in input parameters more obvious. This way the model can be used to simulate real atmospheric situations where the same air mass is measured at two different stations. The distance between the two measurement stations in the model is defined by the user. The upwind measurement site is included in figure 6 as a vertical blue (in 6C white) line. With the addition of a second measurement station the output from the model was also changed. The new output includes one figure for the downwind station as before and also one figure for the upwind station and as well as a figure with both stations for better comparison. The comparison output plot is shown in figure 7.

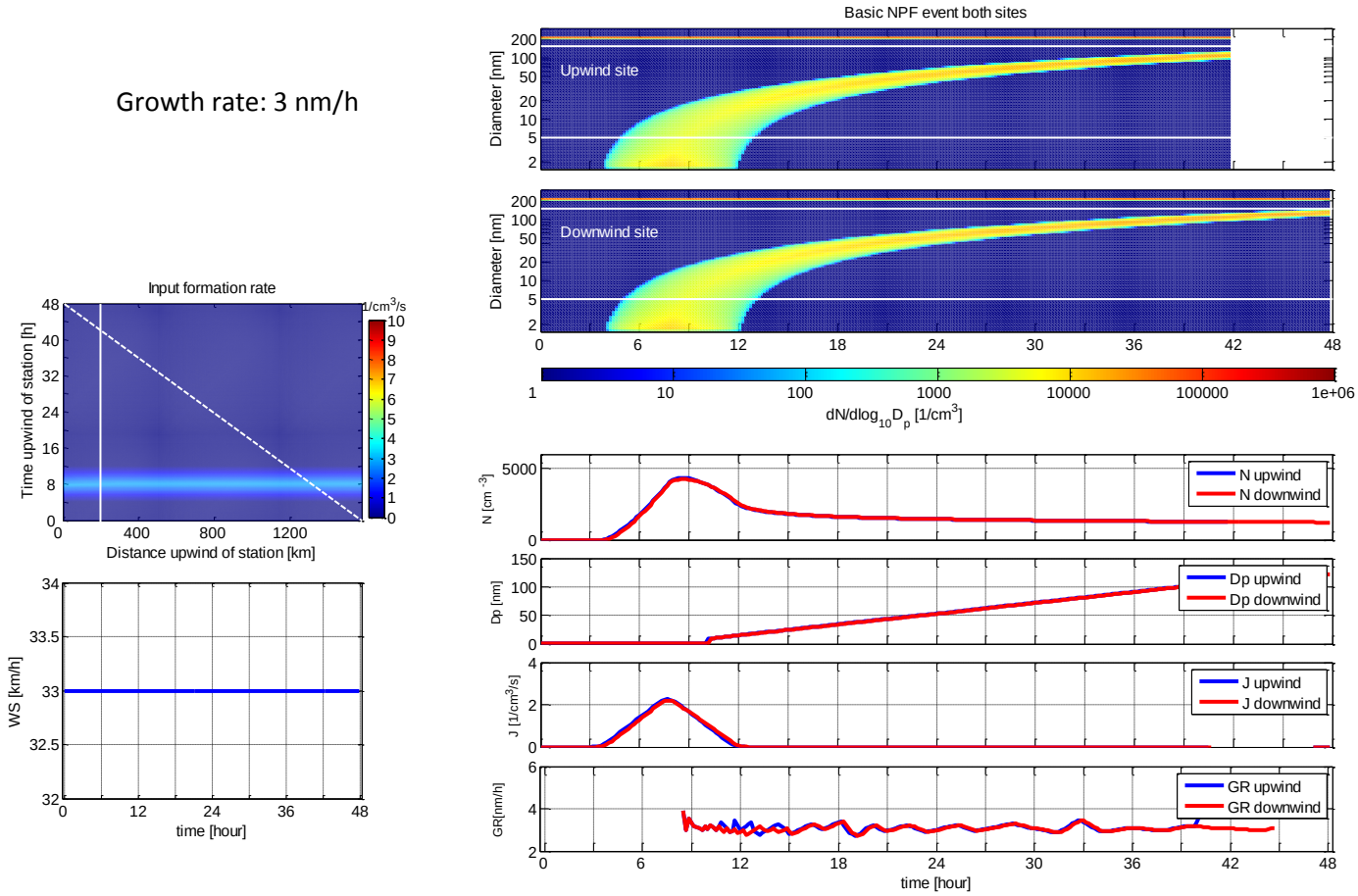

Figure 7: The comparison output of a NPF event simulated with the improved StBanana model. This event is limited only temporally ($J_{1.5}(t)$> 0 between hours 4 and 12 with maximum at 8 hours, all other parameters are constants).Left panels shows input parameters growth rate, formation rate and wind speed. On the right side the two top panels show the evolution of particle number size distribution at both measurement sites as a function of time for two days, with particle number concentrations in each bin given as color in $dN/d\log_{10}D_p$. The third panel shows the number concentration of particles with D_p < 150 nm as a function of time for each site. The fourth panel shows the diameter D_p at both sites as function of time. The fifth panel shows the formation rates, $J_{1.5}$ at both sites as functions, calculated from the output particle number size distribution data. Finally, the bottom panel shows particle growth rates at both sites as functions of time calculated from the output particle number size distribution data.

3.2 Spatial and temporal changes in simulated observations

We simulated 15 cases with different combinations of temporally and spatially changing input formation and growth rates. From the simulation results we identified patterns that were unique to either temporal or spatial changes of the input parameters. The simulation output and these "fingerprints" of the different parameter changes are described below. Our later analysis in this work is limited to banana-type new particle formation events, which require a time-dependent component in the formation rate. For this reason we omit the description of cases with new particle formation rate being only location-dependent (continuous point source).

If particle formation rate changes only as a function of time, the changes in the particle number-size-time plot would occur at the same time at the two measurement sites. These are seen as the beginning and end of time period when new particles appear at 1.5 nm diameter at the two measurement sites in the particle number-size-time plot in figure 7. If the change of new particle formation rate depends also on location the effects of this change are observed at the upwind site earlier than at the downwind site. The delay corresponds to the time it takes for the air to travel between the two sites. This is shown in figure 8 where the upwind site is inside of the formation area and the downwind site is not. The formation of particles starts at 4 hours at the upwind site, but the first particles arrive at the downwind site at 10 hours. The particles grow during the transportation to the downwind site, which is why the banana starts from a larger particle size at the downwind site. The location dependent formation can also be seen in the number concentration, where the particle number concentration is higher at the upwind site in the beginning of the banana. This is because coagulation removes a lot of the smallest particles before they reach the downwind site. The time of last particles to arrive at the two stations also depends on the location dependent formation rate, as the air outside the formation area arrive to the upwind site earlier. This can be seen in the figure where the new particle mode disappears at the upwind site 6 hours earlier than at the downwind site.

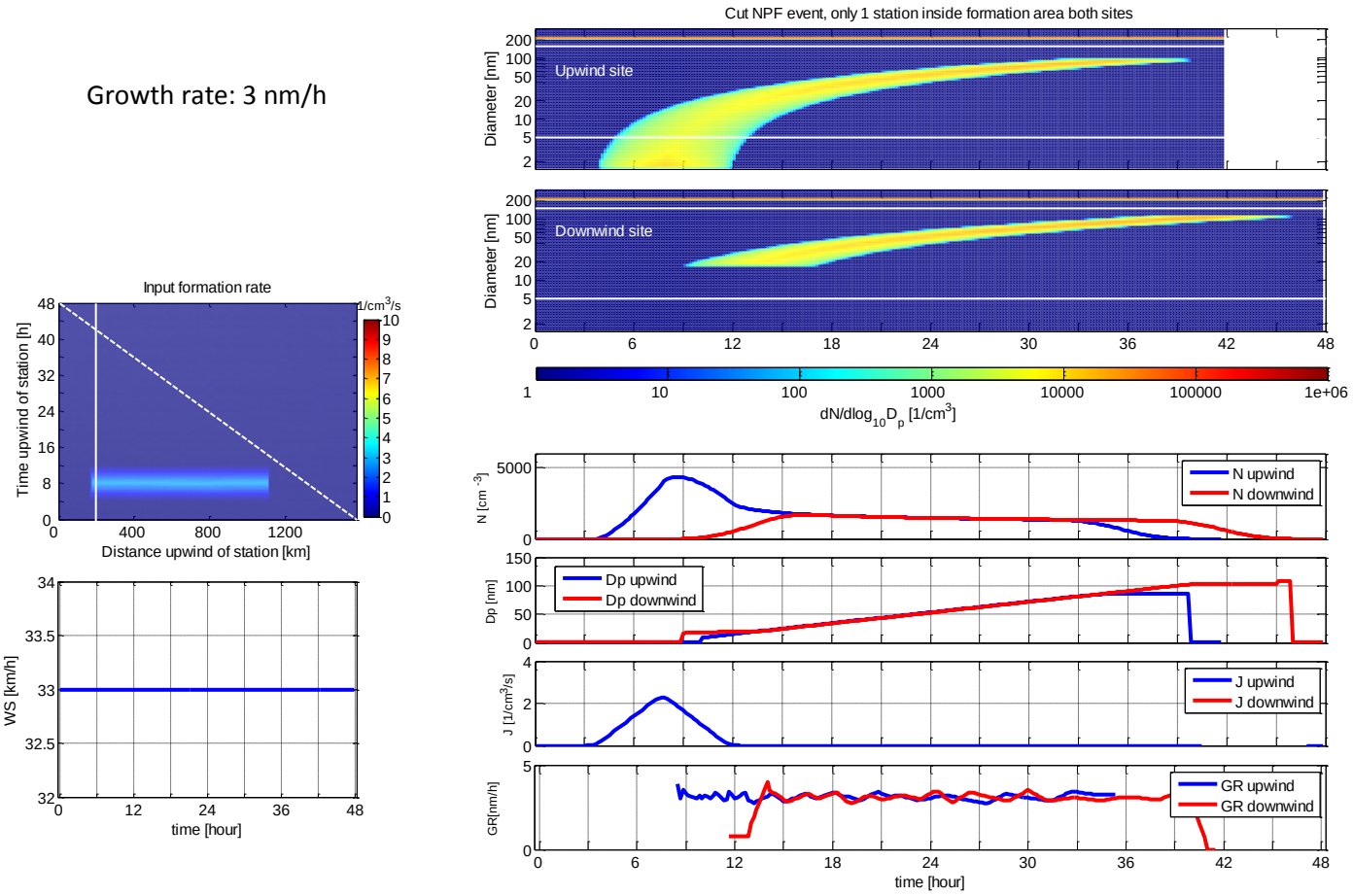

Figure 8: Effects of location dependent change in particle formation rate at two measurement sites. In this example simulation the formation rate of new particles is non-zero 180-1000 km upwind from the downwind site and between 4-12 hours, peaking at 8 hours, and the growth rate is constant at 3 nm/h everywhere and all the time. The distance between the sites is 200 km.

If particle growth rate changes as a function of time, the change occurs in the number-size-time plots at both measurement sites at the same time point. It also does not have any significant effect on the number concentration of particles observed at the sites. If the change of growth rate depends on location instead of time, the effects of this change are observed at the upwind site earlier than at the downwind site. Again the delay corresponds to the time the air mass needs for traveling between the sites. This is demonstrated in figure 9, where the observed particle growth rate drops from 4 nm/h to 2nm/h at 26 hours at the upwind site, but at 32 hours at the downwind site. The location-dependent change in growth rate affects also the observable particle number concentration. This can be explained by the growth rates of particles at the area where they are formed. As coagulation is most efficient in removing the smallest particles, a lower growth rate exposes the particles for the most efficient coagulation for a longer time, and therefore reduces the number of particles that survive to the measurement site. This effect can also be seen in figure 9, and it is explained in more detail in *Kivekäs et al. (2015; 2014).*

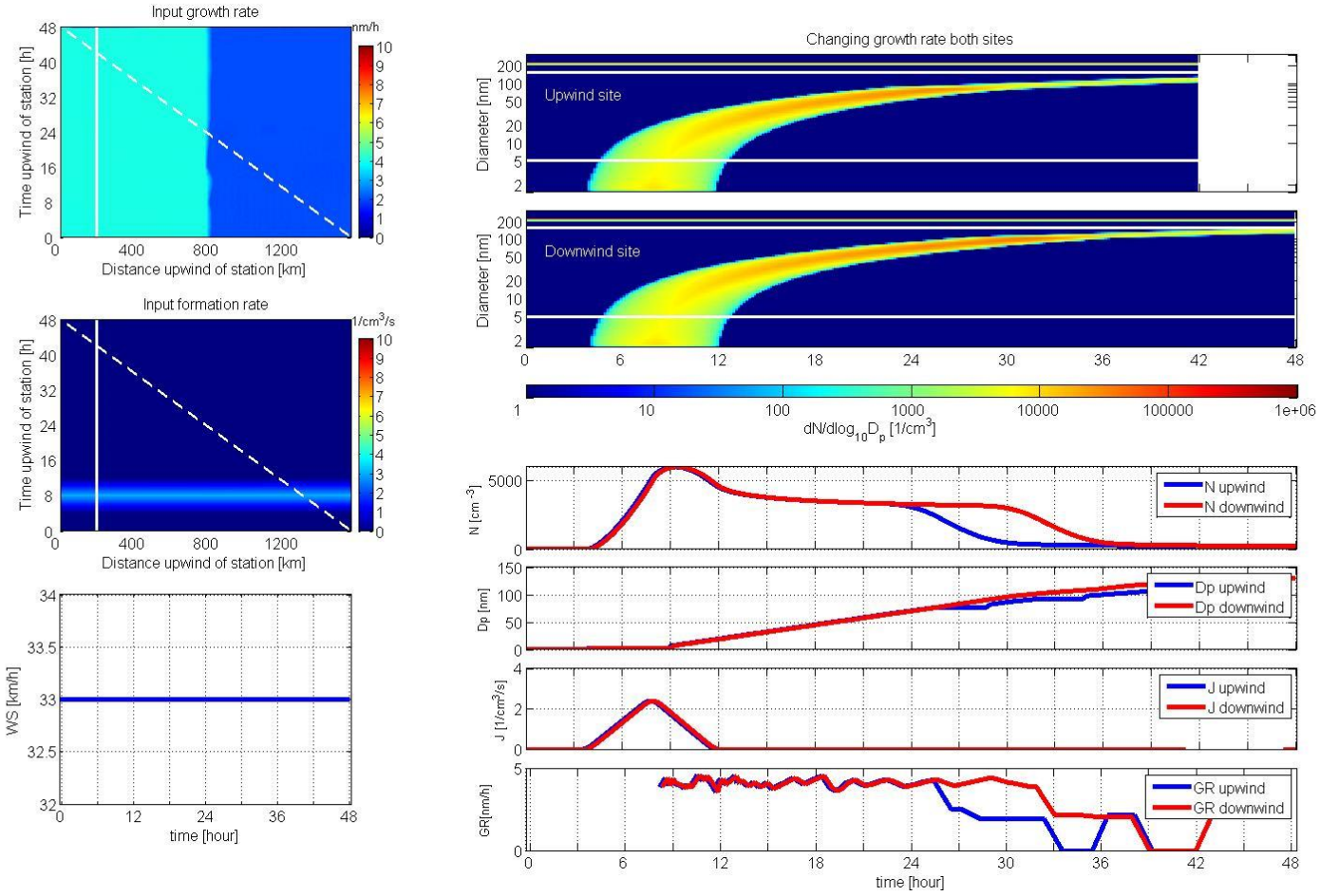

Figure 9: Effects of location dependent change in particle growth rate at two measurement sites. In this example simulation the formation rate of new particles is non-zero everywhere at 4-12 h, peaking at 8h, and the growth rate of particles is 4 nm/h for the first 800 km upwind of the downwind measurement site, and 2 nm/h beyond that.

The effects of time- and location dependent formation and growth rates can be summarized as:

Time dependent formation rate: The beginning and end of time period of appearance of the smallest particles measurable at the site. Both sites are affected simultaneously.

Location dependent formation rate: The beginning, the changing and the ending times of the part of the banana observed at the site. The upwind site is affected before the downwind site.

Time dependent growth rate: Growth rate of the observed mode changes simultaneously at both sites. Particle number concentration in the mode is not affected much.

Location-dependent growth rate: Growth rate of the observed mode changes first at the upwind site. Particle number concentration can be heavily affected by this type of change in GR, and the effect is observed also first at the upwind site.

3.3 Measurement sites

In this work we have analyzed particle number size distribution data from two sites, Pallas and Värriö both located in Finnish Lapland (figure 10). Both of these measurement stations have had continuous particle measurements for roughly two decades. The distance between the stations is approximately 220 km.

Pallas (67.97° N, 24.12°E, 565 m.a.s.l) (*Hatakka et al., 2003*): The Sammaltunturi measurement site at Pallas station is located on a small hill about 300 meters above the surrounding area. The site is located 100 meter above the tree line and the surrounding area is covered by mixed boreal forest consisting of Scots pine, spruce and birch trees. The surrounding area is sparsely populated and there are no significant pollution sources nearby (*Hatakka et al., 2003*).

Värriö (67.77° N, 29.58° E, 390 m.a.s.l.) (*Hari et al., 1994*): The Värriö station has its location on a hilltop and the surrounding area consists of approximately 60 year old Scots pine forest. The site is slightly below the tree line which is 400 m.a.s.l. in the area. There are no local pollution sources in the area. The closest small road is 8 km from the station and the closest major road is 100 km away. The anthropogenic pollution sources are mainly the mining area in Kovdor, Russia and the nickel-copper smelters in Montchegorsk and Nikel, Russia. These are located at a distance of 43 km, 150 km and 190 km, respectively (*Väänänen et al., 2013*).

Figure 10: A map over Scandinavia with Pallas and Värriö measurement stations. Map by Google Earth.

3.4 Trajectories

For the event comparison at Pallas and Värriö we first had to find the cases when the sites were connected by air mass trajectories. In this work HYSPLIT trajectories (*Draxler and Hess, 1998*) arriving at Värriö with 1 hour intervals at 500m altitude above ground level were used. For every air mass trajectory that arrived at Värriö, the minimum distance of the air parcel from Pallas during the previous 24 hours was calculated. If that distance was less than 100 km (figure 11), the air mass was considered as arriving over Pallas, and the particle size distributions of that day at both sites were taken to further analysis. The time difference between the trajectory arrival time at Värriö and the time when it was closest to Pallas represents the time the trajectory has spent travelling from Pallas to Värriö.

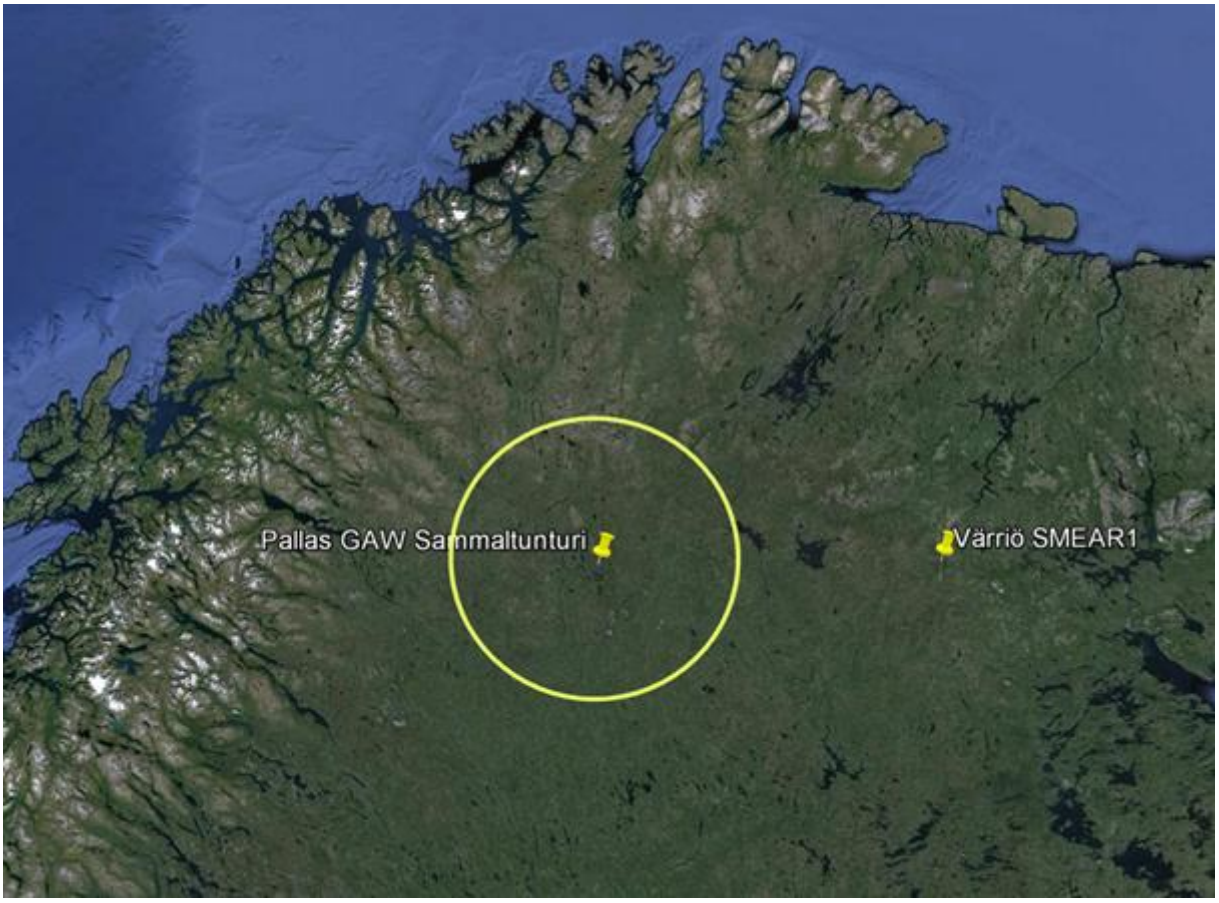

Figure 11: The terrain around Pallas and Värriö measurement stations and the 100 km radius circle for trajectory selection around Pallas station. Map by Google Earth.

3.5 Comparison method

If there was a new particle formation event at Värriö during a day with connecting air mass trajectories, we compared the observed time evolution of particle number size distribution at the two sites visually using the particle number-size-time plots, as well as the calculated values of $N(D_p<100nm)$ and mode peak diameter $D_{p\ peak}$ (figure 12). Due to the fact that the automatic calculation of GR in the real observed events resulted in very much noise we decided to omit it from the analysis and set the value to zero.

The time of connecting trajectories at both sites was also included in the figures for helping us to find whether some clear changes in particle number size distribution happened at the time of the same connecting trajectory at both sites.

The start-times of the analyzed events and the end-times of the growing modes were classified as either time dependent, location dependent or not analyzable. If there were no event at Pallas, the event was classified as one site event. The cases with no event at Värriö are not included the analyzed data set. The definitions of the different fingerprints are given in table 1.

Definitions for the event classification	
Time dependent	Time at Pallas = time at Värriö, ±2 hours
Location dependent	Time at Pallas = time of connecting trajectory, ±2 hours
Not analyzable	Every case not belonging to any other class
One site event	No event at Pallas

Table 1: The definition of how the different types of event start times and end times of the growing mode were classified.

In the case shown in figure 12 there are connecting trajectories for almost the whole time series which makes the analysis more precise. Based on the information obtained from the particle number-size-time plot, the particle number concentration plot and the mode diameter plot the formation starts at 10 hours at Pallas (upwind) and 14 hours at Värriö (downwind). This difference is 4 hours, so the event start is not time dependent. The trajectory arriving at Värriö at time 14 hours was at Pallas at time 6 hours. This differs 4 hours from the event start time at Pallas, so the event start is not location-dependent, either, which results it to be classified as not analyzable. At the end of the banana the last particles of the new mode are observed at Pallas at roughly 22 hours and at Värriö at 28 hours. The trajectory arriving at Värriö at 28 hours was at Pallas at 20 hours, which is within ± 2 hours from the time the last event-related particles were observed at Pallas, making the end of the growing mode (end of event) location dependent.

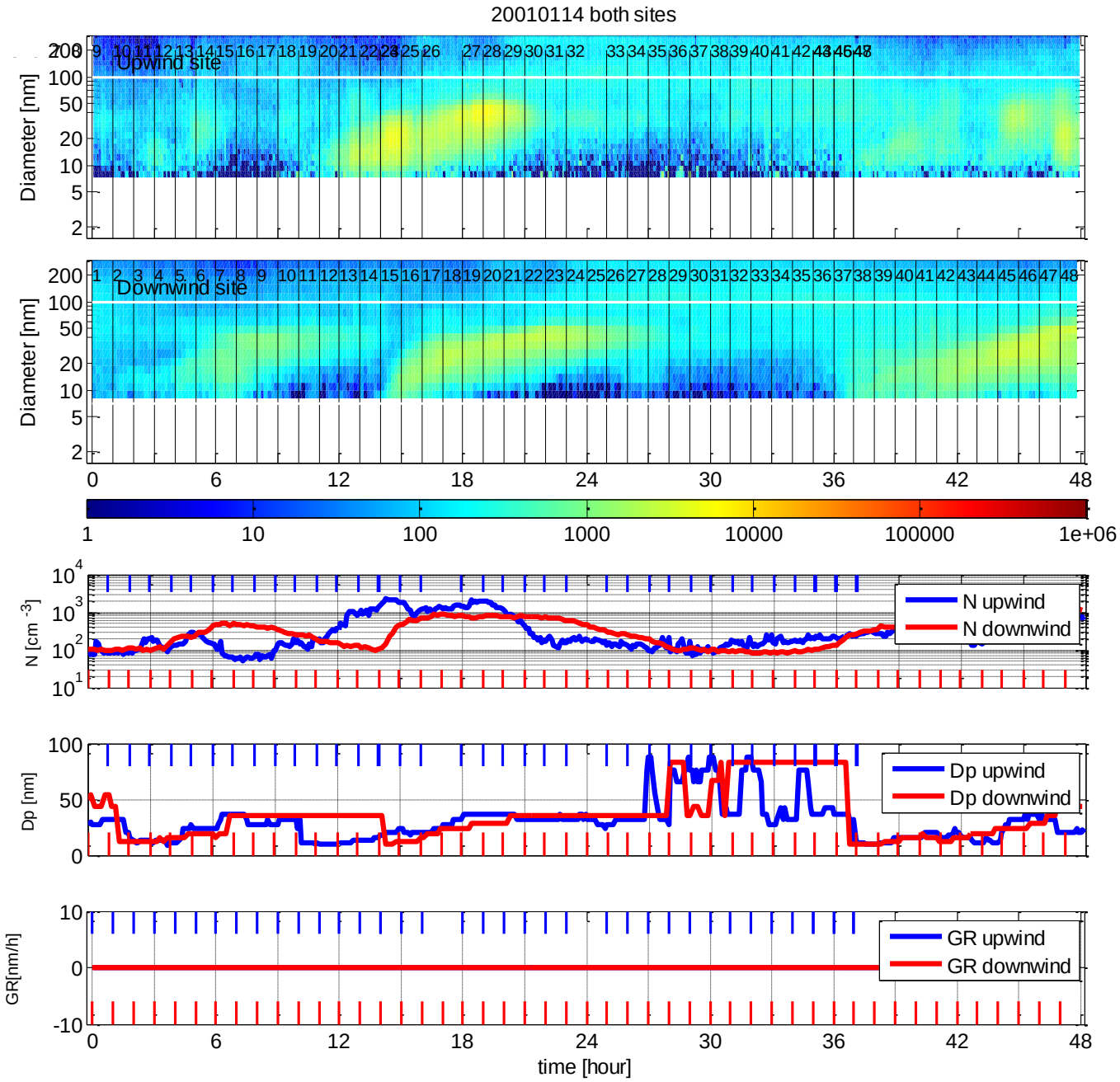

Figure 12: An analyzed event from measurements at Pallas and Värriö the 14th of January 2001. The figure includes 2-day time series of particle number –size-distribution at Pallas (top panel) and at Värriö (2nd panel), number concentration (N) of particles with Dp<100 nm at both sites (3rd panel), mode peak diameter (Dp) of the particles with Dp<100 nm at both sites(4th panel) and the attempt to calculate particle growth rate at both sites (bottom panel) The numbered vertical lines are the times of connecting trajectories identified by the numbers.

4. Results and discussion

After analyzing 8 years of measurements we found 65 cases meeting the two criteria: 1) there had to be a new particle formation event at Värriö during the given day and 2) at least one trajectory during that day had to pass over Pallas before arriving at Värriö. The analysis of the beginning of each event (event start) and end of each observed growth banana (event end) are summarized in table 2, and given in detail in Appendix 1.

Classification of analyzed events								
	Event start				Event end			
	Time-dependent	Location-dependent	Not analyzable	One-site event	Time-dependent	Location-dependent	Not analyzable	One-site event
Total	31	1	21	12	5	10	40	10

Table 2: Summary of the result of the analysis of the NPF events separately for the event starts and event ends.

When we excluded the non-analyzable cases it became obvious that the event start is typically time dependent, whereas the event end tends to be location-dependent (Figure 13). One should keep in mind that if there is an event only at Värriö (one site event), it is also a location dependent phenomenon. The non-analyzable cases are typically either ones with no apparent time dependency and no connecting trajectories at the time of start or end of the event, or cases where the end of the event could not be defined.

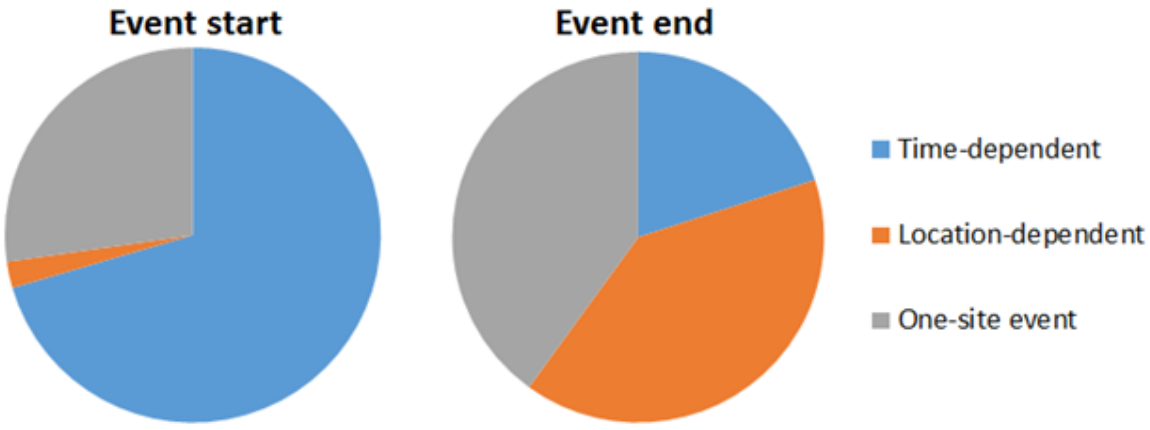

Figure 13: The relative fractions of time dependent, location dependent and one-site events analyzed for event starts and event ends separately.

The typical time dependency of the event start can be explained by the evolution of the turbulent boundary layer (*Asmi et al., 2011*). As sun heats the ground in the morning and around noon the atmospheric turbulence increases in height and the particle-rich air near the ground is mixed with cleaner air above. This leads to a lower condensation sink, allowing the formation of new particles to take place. As the east-west distance between the two stations is only 220 km (5.5 longitude degrees), the sun starts to heat the ground at roughly the same time at both sites.

The event end can be linked to a limited area of particle formation or growth, such as in the simulated cases presented in figures 8 and 9. In real observations in Northern Scandinavia such a limit can be connected to the air mass arriving from sea to land (figure 14) or over the Scandinavian mountains where different vegetation leads to a different source strength of condensable vapors needed for new particle formation. The spatial extent of new particle formation can also be limited by different air mass containing more clouds or higher condensation sink.

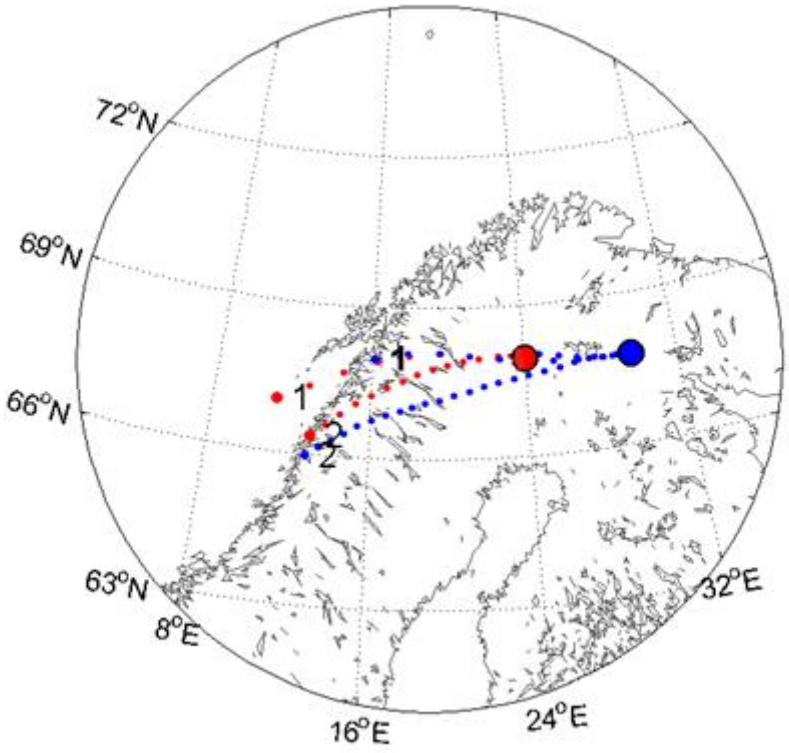

Figure 14: Spatial extent of two new particle formation events in an earlier study (*Kivekäs et al., 2011*) calculated from end of growing mode time and the corresponding trajectories. The largest red and blue dots are the Pallas and Värriö sites, respectively, and the smaller circles are the locations of air mass at each hour in the corresponding trajectories (red for Pallas, blue for Värriö). The numbers next to the furthest trajectory points (end of formation area) connect the trajectories to the two cases.

There are a number of uncertainties in the analysis performed in this work. The simulations are simplified and do not allow different particles to have different growth rates or any mixing of air masses during the transport to the measurement site. Also the air mass arriving route in ambient conditions is never constant for such a long time. These simplifications make the simulation results easier to understand and interpret, but reduce the applicability of the model to simulate real atmospheric observations.

The two-site approach makes the separation between the time-dependent and location-dependent effects in real atmospheric observations more robust, but it introduces another

source of uncertainty: Do the measurements at both sites really represent the same air? In the selection of air mass trajectories we used a radius of 100 km from the Pallas site (figure 11) to determine which trajectories to include in the analysis. The radius is rather long, but it can be justified because NPF is found to be a large scale phenomenon (*Kristensson et al., 2014, Hussein et al., 2009*), the terrain around Pallas station is very homogenous, and the anthropogenic emissions within that area are minor. This means that even if the air mass has not arrived exactly over Pallas, it has been exposed to very similar conditions. A shorter radius would have resulted in higher certainty of measuring the same air mass, but it would have decreased the number of connecting trajectories and therefore made the event analysis weaker.

Finally there is the subjectivity in determining the start- and end times of the events. They can often differ with one or more hour depending on the person performing the analysis, and therefore many individual cases would be classified differently.

Even though the uncertainties can lead to different classification of many of the analyzed new particle formation event, the qualitative main result of this work holds: The observed new particle formation events at Värriö are affected by spatial changes in the formation and / or growth parameters, affecting especially the end of the observed new mode.

5. Conclusions

In case of the events observed at the Värriö measurement station, the beginning of the NPF event is typically time-dependent, but the end of the observed growing mode is often a result of a location-dependent parameter change rather than by a time dependent change. This means that the location-dependency of the formation and growth parameters is an important factor affecting real atmospheric observations of new particle formation events, and that the effects described by *Kivekäs et al. (2015; 2014)* must be taken into account.

Even though the typical analysis of new particle formation events does not require analysis of particles formed hundreds of kilometers away, there can be smaller location dependent variations nearby the site, resulting from vegetation, lakes or other topographic features, and these variations can affect the particle size ranges used for determining the new particle formation rate and the initial growth rate of the particles.

This thesis demonstrates the importance of spatial changes in new particle formation parameters at Värriö, a background site in remote Finnish Lapland with relatively homogenous surrounding topography. It can be expected that such effects are present and potentially more prominent also at other measurement sites with more complex topography and more variable sources of particles and vapors. This description fits to most aerosol measurement sites in Europe. The method used in this study for separating the spatial and temporal changes requires a relatively homogenous particle source area and a second measurement site close to the one studied. The problem with most other sites is that one or both of these requirements is not met, and therefore the effects cannot be identified in the data. This, however, does not mean that they aren't there.

Further research would consist of 1) identifying what causes the location dependent variation in particle formation and growth rates, 2) linking the observed particle growth to growth that takes place at a specific time and location upwind of the site, 3) improving the model by making it spatially 2-dimensional to simulate cases with changing air mass trajectories at individual measurement sites and 4) quantifying the uncertainty caused by spatially varying parameters in parameterizations of particle formation and growth rates at different sites.

6. Acknowledgements

This master thesis was done at the Department of Physical Geography and Ecosystem Science, Lund University. I would like to thank my supervisors Niku Kivekäs at the Atmospheric Composition Research, Finnish Meteorological Institute, Helsinki, Finland and Adam Kristensson at the Department of Nuclear Physics, Lund University for their help and guidance during the work of this thesis. I want to give special thanks to Niku Kivekäs for giving me the opportunity to participate in his research which is in the front of the aerosol research field.

7. References

Ackerman, A.S., Toon O. B., Taylor J. P., Johnson D. W., Hobbs P. V., and Ferek R. J. (2000b). Effects of aerosols on cloud albedo: evaluation of Twomey's parametrization of cloud susceptibility using measurements of ship tracks. *J. Atmos. Sci.*, **57**, 2684–2695.

Albrecht, B. A. (1989). Aerosols, Cloud Microphysics, and Fractional Cloudiness. Science 15 September 1989: Vol. 245 no. 4923 pp. 1227-1230 DOI: 10.1126/science.245.4923.1227.

Asmi, E., Kivekäs, N., Kerminen, V.-M., Komppula, M., Hyvärinen, A.-P., Hatakka, J., Viisanen, Y., and Lihavainen, H. (2011). Secondary new particle formation in Northern Finland Pallas site between the years 2000 and 2010, Atmos. Chem. Phys., 11, 12959-12972, doi:10.5194/acp-11-12959-2011, 2011.

Buringh E. and Opperhuizen A. (Eds.). (2003). On Health Risks of Ambient PM in The Netherlands, RIVM report. This report contains on CD a quite complete evaluation of the present knowledge on the effect of aerosols.

Carpman, J. (2013). Modeling the growth and regional extent of new particle formation events. Department of Nuclear Physics, Lund University, Lund, Sweden. http://www.lunduniversity.lu.se/lup/publication/4004497

Corbrett, J. J., Winebrake, J. J., Green, E. H., Kasibhatla, P., Eyring, V. and Lauer, A. (2007). Mortality from ship emissions: A global assessment. College of Marine and Earth Studies, University of Delaware, 305 Robinson Hall, Newark, Delaware 19716, Department of STS/Public Policy, Rochester Institute of Technology, 1356 Eastman, Rochester, New York 14623, Nicholas School of the Environment, Duke University, Box 90328, Durham, North Carolina 22708, and Deutches Zentrum fuer Luft- und Raumfahrt (DLR) DLR-Institute fuer Physik der Atmosphaere, Oberpfaffenhofen, Wessling, Germany.

Crippa, P. and Pryor, S. C.: Spatial and temporal scales of new particle formation events in eastern North America, Atmos. Environ., 75, 257–264, 2013.

Dal Maso, M., Kulmala, M., Riipinen, I., Wagner, R., Hussein, T., Aalto, P. P. & Lehtinen, K. E. J. (2005). Formation and growth of fresh atmospheric aerosols: eight years of aerosol size distributiondata from SMEAR II, Hyytiälä, Finland. *Boreal Env. Res.* 10: 323–336.

de Leeuw, G., Andreas, E. L., Anguelova, M. D., Fairall, C. W., Lewis, E. R., O'Dowd, C., Schulz, M., and Schwartz, S. E., (2011). Production flux of sea spray aerosol, Rev. Geophys., 49, RG2001, doi:10.1029/2010RG000349.

Draxler, R. R., and Hess, G. D. (1998): An overview of the HYSPLIT_4 modeling system of trajectories, dispersion, and deposition, Aust. Meteor. Mag., 47, 295-308.

Frank, G. (2001). Experimental studies of the interaction of atmospheric aerosol particles with clouds and fogs, ISBN 91-7874-169-6, Doctoral dissertation at Lund University, Dep. of Nuclear physics, Lund, Sweden.

Ginoux, P., Prospero, J. M., Gill, T. E., Hsu, N. C., and Zhao, M., (2012a). Global-scale attribution of anthropogenic and natural dust sources and their emission rates based on MODIS Deep Blue aerosol products. Rev. Geophys., 50, RG3005.

Ginoux, P., Clarisse, L., Clerbaux, C., Coheur, P.-F., Dubovik, O., Hsu, N. C., and Van Damme, M., (2012b). Mixing of dust and NH3 observed globally over anthropogenic dust sources Atmos. Chem. Phys., 12, 7351–7363.

Hari, P., Kulmala, M., Pohja, T., Lahti, T., Siivola, E., Palva, L., Aalto, P., Hämeri, K., Vesala, T., and Luoma, S. (1994): Air pollution in eastern Lapland: challenge for an environmental measurement station, Silva Fenn., 28, 29–39.

Hatakka, J., Aalto, T., Aaltonen, V., Aurela, M., Hakola, H., Komppula, M., Laurila, T., Lihavainen, H., Paatero, J., and Salminen, K. (2003): Overview of the atmospheric research activities and results at Pallas GAW station, Boreal Environ. Res., 8, 365–383.

Haywood, J., and Boucher, O., (2000). Estimates of the direct and indirect radiative forcing due to tropospheric aerosols: A review, Rev. Geophys., 38(4), 513–543, doi:10.1029/1999RG000078.

Hinds, W. C. (1998). Aerosol Technology, New Your, USA, John Wiley & Sons, Inc., 2. edition.

Hinds, W, C. (1999). Aerosol technology: properties, behavior, and measurement of airborne particles.

Huneeus, N., Schulz, M., Balkanski, Y., Griesfeller, J., Prospero, J., Kinne, S., Bauer, S., Boucher, O., Chin, M., Dentener, F., Diehl, T., Easter, R., Fillmore, D., Ghan, S., Ginoux, P., Grini, A., Horowitz, L., Koch, D., Krol, M. C., Landing, W., Liu, X., Mahowald, N.. (2011). Global dust model intercomparison in AeroCom phase I. Atmos. Chem. Phys., 11, 7781-7816, 2011 http://www.atmos-chem-phys.net/11/7781/2011/. doi:10.5194/acp-11-7781-2011.

Hussein, T., Junninen, H., Tunved, P., Kristensson, A., Dal Maso, M., Riipinen, I., Aalto, P. P., Hansson, H.-C., Swietlicki, E., and Kulmala, M. (2009). Times pen and spatial scale of regional new particle formation events over Finland and Southern Sweden. Atmos. Chem. Phys., 9, 4699–4716, 2009 http://www.atmos-chem-phys.net/9/4699/2009/ © Author(s) 2009. This work is distributed under the Creative Commons Attribution 3.0 License.

Ilyinskaya, E., Tsanev, V.I., Martin, R.S., Oppenheimer, C., Le Blond, J., Sawyer, G.M., Gudmundsson, M.T. (2011). Near-source observations of aerosol size distrubutions in the eruptive plumes from Eyjafjallajökull volcano, March-April 2010. doi:10.1016/j.atmosenv.2011.03.017

IPCC, (2001): Climate Change 2001: The Scientific Basis. Contribution of Working Group I to the Third Assessment Report of the Intergovernmental Panel on Climate Change [Houghton, J.T., Ding Y., Griggs D.J., Noguer M., van der Linden P.J., Dai X., Maskell K., and Johnson C.A. (eds.)]. Cambridge University Press, Cambridge, United Kingdom and New York, NY, USA, 881pp.

IPCC (2007). Forster, P., Ramaswamy V., Artaxo P., Berntsen T., Betts R., Fahey D.W., Haywood J., Lean J., Lowe D.C., Myhre G., Nganga J., Prinn R., Raga G., Schulz M. and Van Dorland R., (2007): Changes in Atmospheric Constituents and in Radiative Forcing. In: Climate change 2007: The Physical Science Basis. Contribution of Work Group I to the Fourth Assessment Report of the Intergovernmental Panel on Climate Change. [Solomon, S., Qin D., Manning M., Chen Z., Marquis M., Averyt K.B., Tignor M. and Miller H.L. (eds.)]. Cambridge University Press, Cambridge, United Kingdom and New York, NY, USA.

IPCC (2013). Boucher, O., Randall D., Artaxo P., Bretherton C., Feingold G., Forster P., Kerminen V.-M., Kondo Y., Liao H., Lohmann U., Rasch P., Satheesh S.K., Sherwood S., Stevens B. and Zhang X.Y., 2013: Clouds and Aerosols. In: Climate Change 2013: The Physical Science Basis. Contribution of Working Group I to the Fifth Assessment Report of the Intergovernmental Panel on Climate Change [Stocker, T.F., Qin D., Plattner G.-K., Tignor M., Allen S.K., Boschung J., Nauels A., Xia Y., Bex V. and Midgley P.M. (eds.)]. Cambridge University Press, Cambridge, United Kingdom and New York, NY, USA.

Jacobson, M. Z. (2005), Correction to "Control of fossil-fuel particulate black carbon and organic matter, possibly the most effective method of slowing global warming", J. Geophys. Res., 110, D14105, doi:10.1029/2005JD005888.

Jeong, C.-H., Evans, G. J., McGuire, M. L., Chang, R. Y.-W., Abbatt, J. P. D., Zeromskiene, K., Mozurkewich M., Li, S.-M. and Leaitch, W. R.: Particle formation and growth at five rural and urban sites. Atmos. Chem. Phys., 10, 7979-7995, 2010.

Kerminen, V.-M., Lehtinen, K., Anttila, T. and Kulmala, M. (2004). Dynamics of atmospheric nucleation mode particles: a timescale analysis, *Tellus B*, 56 (2), 135-146.

Kivekäs, N, Asmi, E, Komppula, M, Hyvärinen, A-P, Leppä, J, Virkkula, A, Aalto, P, Nieminen, T, Dal Maso, M, Kulmala, M, Svenningsson, B, Kristensson, A, Arneth, A and Lihavainen, H (2011), Spatial extent of new particle formation events estimated from size distribution and trajectory data, *CRAICC Conference*, 10-13.10.2011, Reykjavik, Iceland.

Kivekäs, N., Carpman, J., Roldin, P., Leppä, J., Kristensson, A., and Asmi, E. (2014), Effect of spatially varying parameters on observations of new particle formation events, *Proceedings of the Finnish Centre of Excellence in Atmospheric Science - From Molecular and Biological processes to The Global Climate Annual Workshop*, 12.–14.11.2014, Helsinki, Finland

Kivekäs N., Carpman J., Roldin P., Leppä J., O'Connor, E., Kristensson A., Asmi E. (2015). Coupling an aerosol box model with one-dimensional flow: a tool for understanding observations of new particle formation events. To be submitted to Tellus B.

Komppula, M., Sihto, S.L., Korhonen, H., Lihavainen, H., Kerminen, V.M., Kulmala, M. &Viisanen, Y. (2006), "New particle formation in air mass transported between two measurement sites in Northern Finland", Atmospheric Chemistry and Physics, vol. 6, no. 10, pp. 2811-2824.

Kristensson, A., Johansson, M., Swietlicki, E., Kivekäs, N., Hussein, T., Nieminen, T., Kulmala, M. & Dal Maso, M. (2014). NanoMap: Geographical mapping of atmospheric new-

particle formation through analysis of particle number size distribution and trajectory data. *Boreal Env. Res.* 19 (suppl. B): 329–342.

Kristensson, A. and Martinsson, B., (2015). The beginner's guide to atmospheric aerosol particles. To be published by Lund University, Lund, Sweden.

Kulmala, M., Vehkämaki, H., Petäjä, T., Dal Maso, M., Lauri, A., Kerminen, V.-M., Birmili, W., and McMurry, P. (2004): Formation and growth rates of ultrafine atmospheric particles: a review of ob- servations, J. Aerosol Sci., 35, 143–176.

Kulmala, M.,Kontkanen, J.,Junninen,H.,Lehtipalo, K.,Manninen, H. E.,Nieminen, T.,Petäjä, T.,Sipilä, M.,Schobesberger, S.,Rantala, P.,Franchin, A.,Jokinen, T., Järvinen, E.,Äijälä, M.,Kangasluoma, J.,Hakala, J., Aalto, P. P., Paasonen,P.Mikkilä, J.,Vanhanen, J., Aalto, J.,Hakola, H., Makkonen, U.,Ruuskanen, T., Mauldin III, R. L.,Duplissy, J., Vehkamäki, H.,Bäck, J.,Kortelainen, A.,Riipinen, I.,Kurtén, T., Johnston, M. V., Smith, J. N.,Ehn, M.,Mentel, T. F., Lehtinen, K. E. J.,Laaksonen, A.,Kerminen, V-M.,Worsnop, D. R., (2013). Direct Observations of Atmospheric Aerosol Nucleation. *Science* **339**, 943 (2013); DOI: 10.1126/science.1227385

Kyrö, E.-M., Kerminen, V.-M., Virkkula, A., Dal Maso, M., Parshintsev, J., Ruíz-Jimenez, J., Forsström, L., Manninen, H. E., Riekkola, M.-L., Heinonen, P., and Kulmala, M. (2013): Antarctic new particle formation from continental biogenic precursors, Atmos. Chem. Phys. Discuss., 12, 32741-32794, doi:10.5194/acpd-12-32741-2012.

Leaitch, W. R., and Isaac, G. A. (1991). Tropospheric aerosol size distributions from 1982 to 1988 over Eastern North America, Atmos. Environ. 25A, 601-619.

Lehtinen, K.E.J., Dal Maso, M., Kulmala, M. and Kerminen, V.-M.. (2007). Estimating nucleation rates from apparent particle formation rates and vice versa: Revised formulation of the Kerminen–Kulmala equation, J. Aerosol Sci., 38 (9),pp 988–994, DOI: 10.1016/j.jaerosci.2007.06.009.

Leppä, J., Anttila, T., Kerminen, V.-M., Kulmala, M., and Lehtinen, K. E. J. (2011). Atmospheric new particle formation: real and apparent growth of neutral and charged particles. Atmos. Chem. Phys., 11, 4939–4955, 2011 http://www.atmos-chem-phys.net/11/4939/2011/ doi:10.5194/acp-11-4939-2011 © Author(s) 2011. CC Attribution 3.0 License.

Linak, W.P., Yoo, J-I., Wasson, S.J., Zhu, W., Wendt, J.O.L., Huggins, F.E., Chen, Y., Shah, N., Huffman, G.P., Gilmour, M.I. (2006). Ultrafine ash aerosols from coal combustion: Characterization and health effects. doi:10.1016/j.proci.2006.08.086

McCormick, M.P., Thomason, L.,W. and Trepte, C.R. (1995), Atmospheric effects of the Mt Pinatubo eruption, *Nature* 373, 399-404 (2 February 1995) | doi:10.1038/373399a0

Miller, R., Morcrette, J.-J., Myhre, G., Penner, J., Perlwitz, J., Stier, P., Takemura, T., and Zender, C. S., (2011). Global dust model intercomparison in AeroCom phase I, Atmos. Chem. Phys., 11, 7781-7816, doi:10.5194/acp-11-7781-2011.

Penner, J. E., Andreae, M., Annegarn, H., Barrie, L., Feichter, J., Hegg, D., Jayaraman, A., Leaitch, R., Murphy, D., Nganga, J., and Pitari, G. (2001). Aerosols, their Direct and Indirect Effects, in: Climate Change 2001: The Scientific Basis, edited by: Houghton, J. T., Ding, Y., Griggs, D. J., Noguer, M., Van der Linden, P. J., Dai, X., Maskell, K., and Johnson, C. A., Report to Intergovernmental Panel on Climate Change from the Scientific Assessment Working Group (WGI), Cambridge University Press, 289–416,

Pincus, R., Baker, M. B. (1994). Effect of precipitation on the albedo susceptibility of clouds in the marine boundary layer. *Nature*, 17 November 1994 Volume 372, pages 250-252. doi:10.1038/372250a0

Putaud, J. P., Raes, F., Van Dingenen, R., Bruggemann, E., Facchini, M., Decesari, S., ... & Wiedensohler, A. (2004). A European aerosol phenomenology—2: chemical characteristics of particulate matter at kerbside, urban, rural and background sites in Europe. Atmospheric Environment, 38(16), 2579-2595.

Rayes, M., (1997). GISS IPC: Aerosols in the atmosphere. National Aeronautics and Space Administration. Goddard Institute for Space Studies. http://icp.giss.nasa.gov/research/ppa/1997/reyes/

Samet J. M., Zeger, S. L., Dominici, F., Curriero, F., Coursac, I., Dockery, D. W., Schwartz, J., Zanobetti, A., (2000) Res. Rpt. - Health Eff. Inst. n94, Part II.

Seinfeld, J. H., Pandis, S. N., (2006). Atmospheric chemistry and physics: From air pollution to climate change – 2nd edition.

Slanina, S., (2012). Impact of local air pollution. Retrieved from http://www.eoearth.org/view/article/153774

Strutt, J., (1871). On the scattering of light by small particles. Philosophical Magazine, series 4, vol 41, pages 447-454.

Tunved, P., Hansson, H.-C., Kerminen, V.-M., Ström, J., Dal Maso, M., Lihavainen, H., Viisanen, Y., Aalto, P.P., Komppula, M., and Kulmala, M., (2006). High natural aerosol loading over boreal forests, Science, Vol. 312 no. 5771 pp. 261-263, *DOI:* 10.1126/science.1123052.

Twomey, S., (1974). Pollution and the planetary albedo. Atmospheric Environment Vol. 8. Pp. 1251-1256. Pergamon Press 1974.

Väänänen R., Kyrö E.-M., Nieminen T., Kivekäs N., Junninen H., Virkkula A., Dal Maso M., Lihavainen H., Viisanen Y., Svenningsson B., Holst T., Arneth A., Aalto P. P., Kulmala M., and Karminen V.-M., (2013). Analysis of particle size distribution changes between three measurement sites in northern Scandinavia. Atmos. Chem. Phys., 13, 11887–11903, 2013 http://www.atmos-chem-phys.net/13/11887/2013/ doi:10.5194/acp-13-11887-2013

Wallace, J. M., and Hobbs, P. V., (2006). Atmospheric Science; An Introductory Survey. Elsevier. Second Edition.

World Air Quality Index. (2015). http://waqi.info/

Yue, D. I., Hu, M., Zhang, R. Y., Wang, Z. B., Zheng, J., Wu, Z. J., Wiedensohler, A., He, L. Y., Huang, X. F. and Zhu, T., (2010). The roles of sulfuric acid in new particle formation and growth in the mega-city of Beijing. Atmos. Chem. Phys., 10, 4953–4960, 2010 www.atmos-chem-phys.net/10/4953/2010/ doi:10.5194/acp-10-4953-2010.

Zhang, R., Khalizov, A., Wang, L., Hu, M., & Xu, W., (2011). Nucleation and Growth of Nanoparticles in the Atmosphere.Chemical Reviews, 112(3), 1957-2011.

9. Appendix 1: Classification of individual NPF events

Table A1.1. Classification of the event start for each analyzed new particle formation event.

Start of event						
Date	Time at Pallas	Time at Värriö	Time-dependent	Location-dependent	Not analyzable	One-site event
2000-04-27	11	13	X			
2000-05-08		11				X
2000-05-09	12	11	X			
2000-05-10	13	12	X			
2000-05-13	11	13	X			
2000-10-23	16	15	X			
2001-01-14	10	14			X	
2001-01-15		12				X
2001-01-16	15	17	X			
2001-01-18		1				X
2001-02-16					X	
2001-04-20	13	14	X			
2001-04-21	10	12	X			
2001-05-04	11	11	X			
2001-05-05	11	11	X			
2001-05-07	10	13			X	
2001-07-03	9	15		X		
2001-09-26		20				X
2002-01-12	12	12	X			
2002-03-29					X	
2002-04-07		20				X
2002-04-11	12	12	X			
2002-04-21	11	12	X			
2002-05-04	13	18			X	
2002-07-30		9				X
2002-08-06						X
2002-08-29	10	16			X	
2003-03-11					X	
2003-03-23					X	
2003-03-27					X	
2003-04-01	16	15	X			
2003-05-08	13	11	X			
2003-09-15	14	15	X			
2003-12-02					X	
2004-04-02					X	
2004-04-12	12	12	X			
2004-06-03					X	
2004-11-08	16	12			X	
2005-04-24	17	11			X	

2005-04-25	11	14			X	
2005-07-12		8				X
2005-07-14	9	7	X			
2006-01-16	11	13	X			
2006-03-13					X	
2006-05-15	13	13	X			
2006-06-11	12	14	X			
2006-06-16	6	8	X			
2006-09-11					X	
2006-09-15		13				X
2006-12-21	7	7	X			
2007-03-12	16	15	X			
2007-03-21	21	15			X	
2007-03-31	14	14	X			
2007-04-05					X	
2007-04-09	15	16	X			
2007-04-14					X	
2007-04-17		9				X
2007-04-22	11	12	X			
2007-07-21	12	12	X			
2007-08-06		9				X
2007-12-19					X	
2008-04-17	10	11	X			
2008-04-20	12	12	X			
2008-04-21	12	12	X			
2008-05-10		10				X

Table A1.2. Classification of the event end for each analyzed new particle formation event.

End of event						
Date	Time at Pallas	Time at Värriö	Time-dependent	Location-dependent	Not analyzable	One-site event
2000-04-27	39	41	X			
2000-05-08		22				X
2000-05-09	34	41		X		
2000-05-10	19	31			X	
2000-05-13		23			X	
2000-10-23					X	
2001-01-14	22	28		X		
2001-01-15		32				X
2001-01-16	22	27		X		
2001-01-18		15				X
2001-02-16					X	
2001-04-20	19	38			X	
2001-04-21	35				X	

2001-05-04	20	30		X		
2001-05-05	22	33		X		
2001-05-07	20	27			X	
2001-07-03	21	36		X		
2001-09-26		36				X
2002-01-12					X	
2002-03-29					X	
2002-04-07		33				X
2002-04-11		36		X		
2002-04-21	19	24			X	
2002-05-04	23	33			X	
2002-07-30		19				X
2002-08-06						X
2002-08-29	38	42			X	
2003-03-11					X	
2003-03-23					X	
2003-03-27					X	
2003-04-01					X	
2003-05-08	20	31		X		
2003-09-15	28	30	X		X	
2003-12-02					X	
2004-04-02					X	
2004-04-12		33			X	
2004-06-03					X	
2004-11-08	38	44			X	
2005-04-24	24	34			X	
2005-04-25	23	32			X	
2005-07-12					X	
2005-07-14	24	33			X	
2006-01-16	21	27			X	
2006-03-13					X	
2006-05-15	23	27			X	
2006-06-11	20	32				
2006-06-16	19	42			X	
2006-09-11					X	
2006-09-15					X	
2006-12-21	21	33			X	
2007-03-12	42	44	X			
2007-03-21		38			X	
2007-03-31	25	26	X			
2007-04-05					X	
2007-04-09					X	
2007-04-14					X	
2007-04-17		30				X
2007-04-22					X	

2007-07-21	23	31		X		
2007-08-06		17				X
2007-12-19					X	
2008-04-17	22	33			X	
2008-04-20	36	35	X			
2008-04-21	27	37		X		
2008-05-10		26				X

Table 4: Detailed analysis of the end of each observed growth banana.

Institutionen för naturgeografi och ekosystemvetenskap, Lunds Universitet.

Student examensarbete (Seminarieuppsatser). Uppsatserna finns tillgängliga på institutionens geobibliotek, Sölvegatan 12, 223 62 LUND. Serien startade 1985. Hela listan och själva uppsatserna är även tillgängliga på LUP student papers (www.nateko.lu.se/masterthesis) och via Geobiblioteket (www.geobib.lu.se)

The student thesis reports are available at the Geo-Library, Department of Physical Geography and Ecosystem Science, University of Lund, Sölvegatan 12, S-223 62 Lund, Sweden. Report series started 1985. The complete list and electronic versions are also electronic available at the LUP student papers (www.nateko.lu.se/masterthesis) and through the Geo-library (www.geobib.lu.se)

315 Emelie Norhagen (2014) Växters fenologiska svar på ett förändrat klimat - modellering av knoppsprickning för hägg, björk och asp i Skåne
316 Liisi Nõgu (2014) The effects of site preparation on carbon fluxes at two clear-cuts in southern Sweden
317 Julian Will (2014) Development of an automated matching algorithm to assess the quality of the OpenStreetMap road network - A case study in Göteborg, Sweden
318 Niklas Olén (2011) Water drainage from a Swedish waste treatment facility and the expected effect of climate change
319 Wösel Thoresen (2014) Burn the forest - Let it live. Identifying potential areas for controlled forest fires on Gotland using Geographic Information System
320 Jurgen van Tiggelen (2014) Assimilation of satellite data and in-situ data for the improvement of global radiation maps in the Netherlands.
321 Sam Khallaghi (2014) Posidonia Oceanica habitat mapping in shallow coastal waters along Losinj Island, Croatia using Geoeye-1 multispectral imagery.
322 Patrizia Vollmar (2014) The influence of climate and land cover on wildfire patterns in the conterminous United States
323 Marco Giljum (2014) Object-Based Classification of Vegetation at Stordalen Mire near Abisko by using High-Resolution Aerial Imagery
324 Marit Aalrust Ripel (2014) Natural hazards and farmers experience of climate change on highly populated Mount Elgon, Uganda
325 Benjamin Kayatz (2014) Modelling of nitrous oxide emissions from clover grass ley – wheat crop rotations in central eastern Germany - An application of DNDC
326 Maxime Rwaka (2014) An attempt to investigate the impact of 1994 Tutsi Genocide in Rwanda on Landscape using Remote Sensing and GIS analysis
327 Ruibin Xu (2014) Spatial analysis for the distribution of cells in tissue sections
328 Annabelle Finck (2014) Bird biodiversity in relation to forest composition in Sweden
329 Tetiana Svystun (2015) Modeling the potential impact of climate change on the distribution of Western Corn Rootworm in Europe”

330 Joel Forsmoo (2014) The European Corn Borer in Sweden: A Future Perspective Based on a Phenological Model Approach

331 Andrew Ekoka Mwambo (2015) Estimation of Cropland Ecological Footprint within Danish Climate Commissions 2050 Scenarios for Land use and Bioenergy Consumption

332 Anna Lindstein (2015) Land- atmosphere exchange of carbon dioxide in a high Arctic fen: importance of wintertime fluxes

333 Karla Susana Markley Vergara (2015) Present and near future water availability for closing yield gaps in four crops in South America

334 Klara Århem & Fredrik Fredén (2015) Land cover change and its influence on soil erosion in the Mara region, Tanzania: Using satellite remote sensing and the Revised Universal Soil Loss Equation (RUSLE) to map land degradation between 1986 and 2013

335 Fei Lu (2015) Compute a Crowdedness Index on Historical GIS Data- A Case Study of Hög Parish, Sweden, 1812-1920

336 Lina Allesson (2015) Impact of photo-chemical processing of dissolved organic carbon on the bacterial respiratory quotient in aquatic ecosystems

337 Andreas Kiik (2015) Cartographic design of thematic polygons: a comparison using eye-movement metrics analysis

338 Iain Lednor (2015) Testing the robustness of the Plant Phenology Index to changes in temperature

339 Louise Bradshaw (2015) Submerged Landscapes - Locating Mesolithic settlements in Blekinge, Sweden

340 Elisabeth Maria Farrington (2015) The water crisis in Gaborone: Investigating the underlying factors resulting in the 'failure' of the Gaborone Dam, Botswana

341 Annie Forssblad (2015) Utvärdering av miljöersättning för odlingslandskapets värdefulla träd

342 Iris Behrens, Linn Gardell (2015) Water quality in Apac-, Mbale- & Lira district, Uganda - A field study evaluating problems and suitable solutions

343 Linnéa Larsson (2015) Analys av framtida översvämningsrisker i Malmö - En fallstudie av Castellums fastigheter

344 Ida Pettersson (2015) Comparing Ips Typographus and Dendroctonus ponderosas response to climate change with the use of phenology models

345 Frida Ulfves (2015) Classifying and Localizing Areas of Forest at Risk of Storm Damage in Kronoberg County

346 Alexander Nordström (2015) Förslag på dammar och skyddsområde med hjälp av GIS: En studie om löv- och klockgroda i Ystad kommun, Skåne

347 Samanah Seyedi-Shandiz (2015) Automatic Creation of Schematic Maps - A Case Study of the Railway Network at the Swedish Transport Administration

348 Johanna Andersson (2015) Heat Waves and their Impacts on Outdoor Workers – A Case Study in Northern and Eastern Uganda

349 Jimmie Carpman (2015) Spatially varying parameters in observed new particle formation events